Supporting information

Photophysical and electroluminescent properties of bis(2′,6′-difluoro-2,3′-bipyridinato-N,C4′)iridium(picolinate) complexes: effect of electron-withdrawing and electron-donating group substituent at the 4′ position on the pyridyl moiety of the cyclometalated ligand

K. S. Bejoymohandas,[a, b] Arunandan Kumar,[c] S. Varughese,[a] E. Varathan,[d] V. Subramanian[d] and M. L. P. Reddy*[, a, b]

[a]Materials Science and Technology Division, CSIR-Network of Institutes for Solar Energy, CSIR-National Institute for Interdisciplinary Science & Technology (CSIR-NIIST), Thiruvananthapuram-695 019, India

[b]Academy of Scientific and Innovative Research (AcSIR), New Delhi 110001, India

[c]Laboratoire Interdisciplinaire Carnot de Bourgogne (ICB) UMR 6303 CNRS, Université de Bourgogne. 9, Av. Savary, BP 47870, 21078 Dijon Cedex, France.

[d]Chemical Laboratory, CSIR-Central Leather Research Institute, Chennai – 600 020, India

*Corresponding author: E-mail: mlpreddy55@gmail.com

Contents

Fig. S21 MALDI-TOF spectrum of complex **Ir3**.

Fig. S22 ^{1}H-NMR spectrum of 2',6'-difluoro-4-methoxy-2,3'-bipyridine (**L4**).

Fig. S23 ^{13}C-NMR spectrum of 2',6'-difluoro-4- methoxy-2,3'-bipyridine (**L4**).

Fig. S24 ^{19}F-NMR spectrum of 2',6'-difluoro-4- methoxy-2,3'-bipyridine (**L4**).

Fig. S25 ESI-MS spectrum of 2',6'-difluoro-4- methoxy-2,3'-bipyridine (**L4**).

Fig. S26 ^{1}H-NMR spectrum of complex **Ir4.**

Fig. S27 ^{19}F-NMR spectrum of complex **Ir4.**

Fig. S28 MALDI-TOF spectrum of complex **Ir4**.

Fig. S29 ^{1}H-NMR spectrum of 2-bromo-4-N,N-dimethylaminopyridine (**L5a**).

Fig. S30 ^{13}C-NMR spectrum of 2-bromo-4-N,N-dimethylaminopyridine (**L5a**).

Fig. S31 ESI-MS spectrum of 2-bromo-4-N,N-dimethylaminopyridine (**L5a**).

Fig. S32 ^{1}H-NMR spectrum of 2',6'-difluoro-4-(N,N-dimethylamine)-2,3'-bipyridine (**L5**).

Fig. S33 ^{13}C-NMR spectrum of 2',6'-difluoro-4-(N,N-dimethylamine)-2,3'-bipyridine (**L5**).

Fig. S34 ^{19}F-NMR spectrum of 2',6'-difluoro-4-(N,N-dimethylamine)-2,3'-bipyridine (**L5**).

Fig. S35 ESI-MS spectrum of 2',6'-difluoro-4-(N,N-dimethylamine)-2,3'-bipyridine (**L5**).

Fig. S36 ^{1}H-NMR spectrum of complex **Ir5.**

Fig. S37 ^{19}F-NMR spectrum of complex **Ir5.**

Fig. S38 MALDI-TOF spectrum of complex **Ir5**.

Fig. S39 General structure of the complexes shows the label used for selected atoms as used in Table 2.

Fig. S40 Thermogravimetric curves for complex **Ir1 Ir5** under N_2 atmosphere.

Fig. S41 Differential scanning calorimetric curves for complex **Ir1–Ir5** under N_2 atmosphere.

Fig. S42 Optimized geometrical structures of complex **Ir1** **Ir5**.

Fig. S43 Comparison of reduction potentials (vs Ag/AgCl in CH_3CN) of **Ir1** **Ir5**,

Fig. S44 Comparison of oxidation potentials (vs Ag/AgCl in CH_3CN) of **Ir1** **Ir5**, (oxidation potential $FeCp_2/FeCp_2^+$ =0.45 V, marked with asterisk).

Fig. S45 Lifetime decay profiles of complex **Ir1** **Ir5** in degassed dichloromethane solution (c = 5×10^{-5} M, λ_{exc} = 375 nm) at 298 K.

Fig. S46 Lifetime decay profiles of complex **Ir1** **Ir5** in 5 wt% doped PMMA film (λ_{exc} = 375 nm) at 298 K.

Table S1 Selected Bond Lengths for Complexes **Ir2** and **Ir4**

Table S2 Selected Bond Angles for Complexes **Ir2**

Table S3 Selected Bond Angles for Complexes **Ir4**

Table S4 Intermolecular Hydrogen Bond Interactions for **Ir2**

Table S5 Intermolecular Hydrogen Bond Interactions for **Ir4**

Table S6 Selected Bond Distances, Bond Angles and Dihedral Angles from the Optimized Ground ($\mathbf{S_0}$) and Triplet State ($\mathbf{T_1}$) Geometry for the Complexes **Ir1** **Ir5** Together with the Experimental Values for **Ir2** and **Ir4**

Table S7 Calculated energy levels of the HOMO, HOMO-1, HOMO-2, LUMO, LUMO+1, and LUMO+2 and Percentage of Contribution of Iridium metal (Ir), 2′,6′-difluoro-2,3′-bipyridine Derivatives and Picolinate (pic) Ligands

Table S8 Calculated Absorption of **Ir1** **Ir5** in CH_2Cl_2 Media at TD-B3LYP Level together with Experimental Values

Table S9 Calculated singlet-triplet splitting energy at the B3LYP/6-31G* level

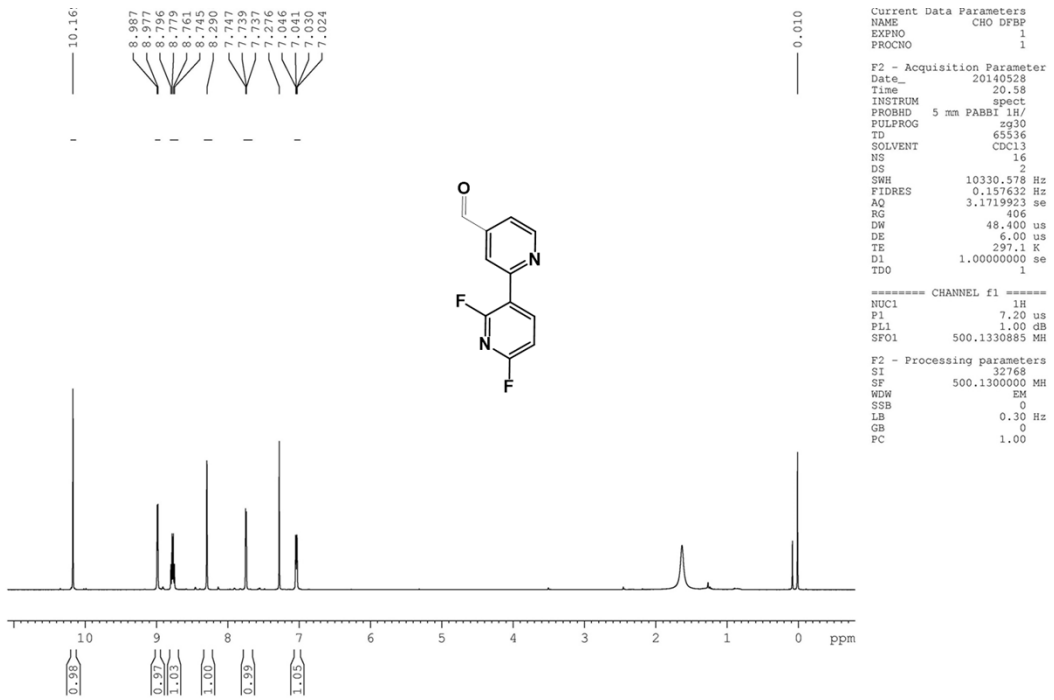

Fig. S1 [1]H-NMR spectrum of 2',6'-difluoro-4-(formyl)-2,3'-bipyridine (**L1**).

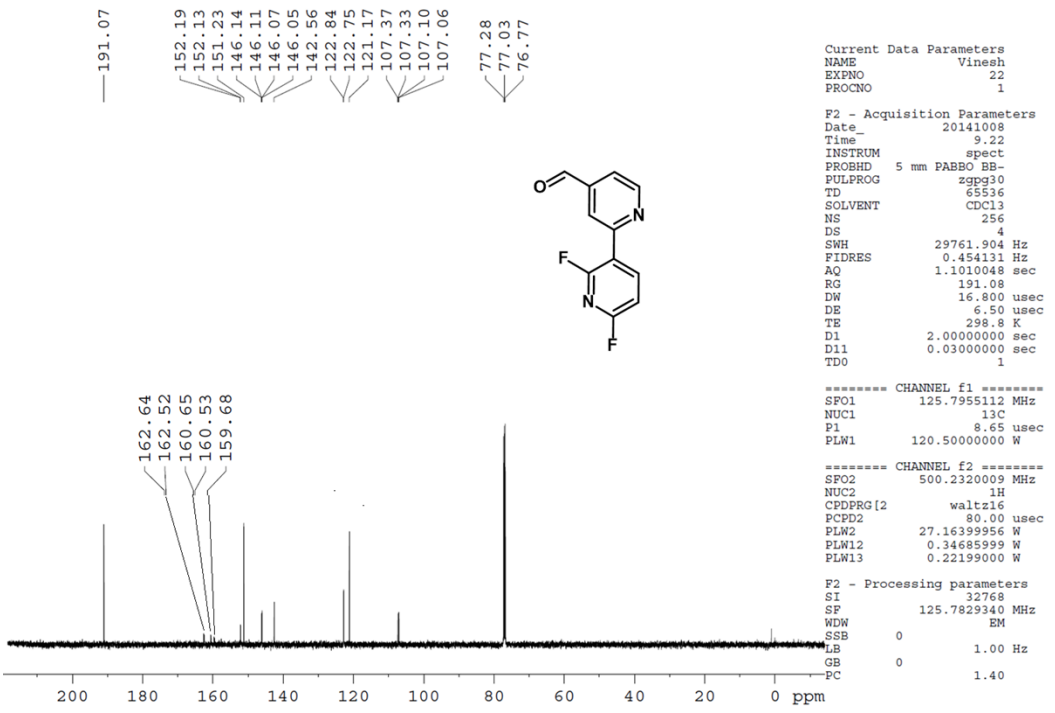

Fig. S2 [13]C-NMR spectrum of 2',6'-difluoro-4-(formyl)-2,3'-bipyridine (**L1**).

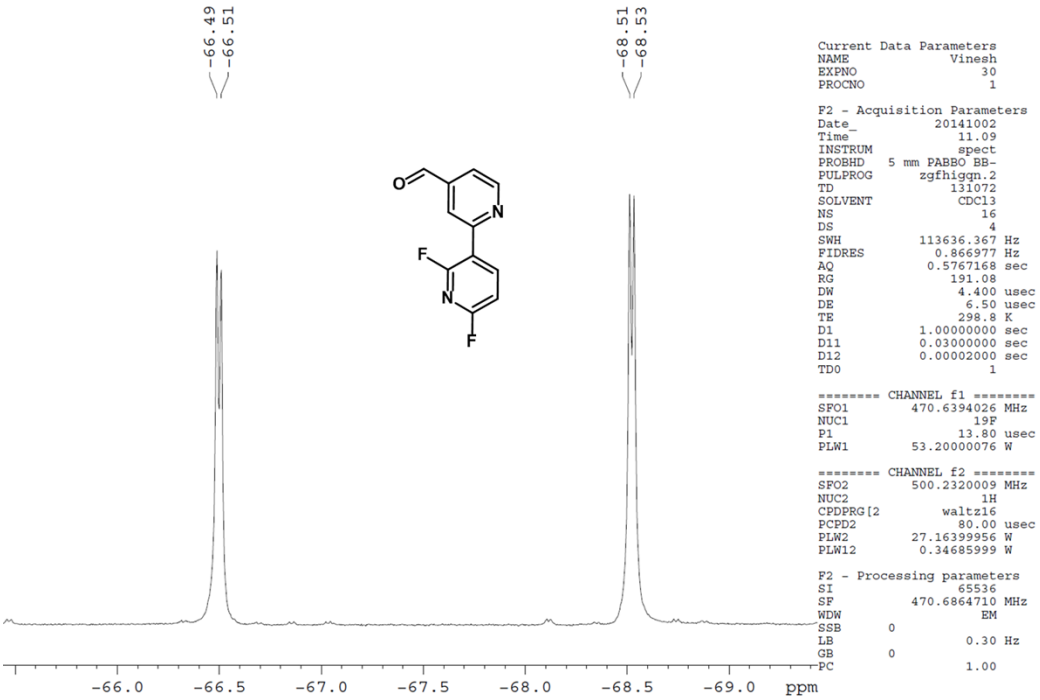

Fig. S3 ^{19}F-NMR spectrum of 2',6'-difluoro-4-(formyl)-2,3'-bipyridine (**L1**).

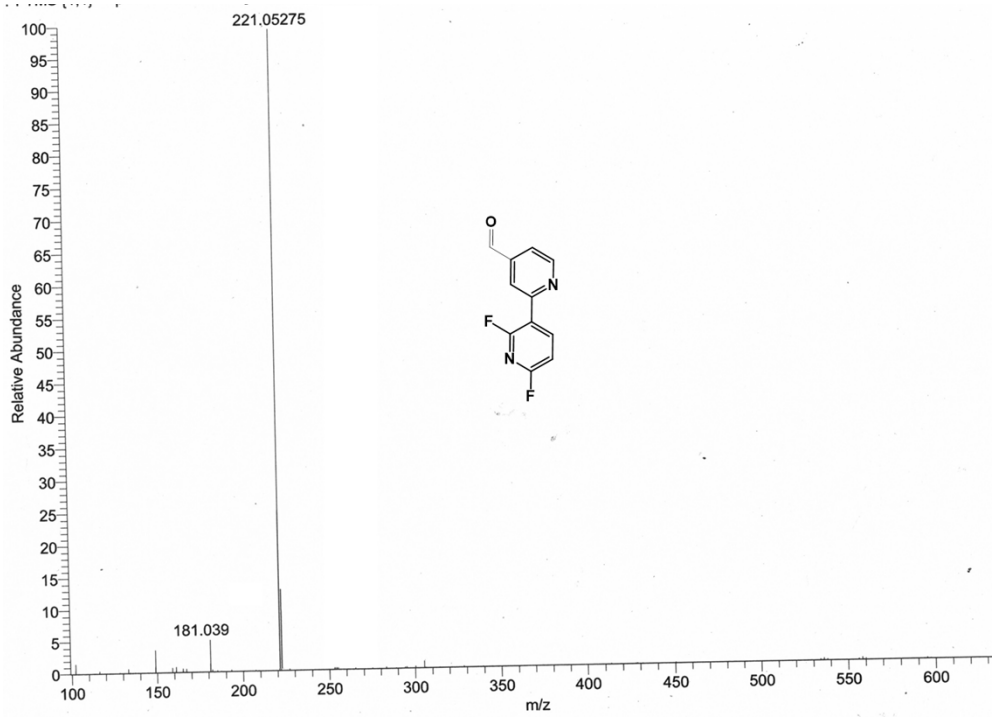

Fig. S4 ESI-MS spectrum of 2',6'-difluoro-4-(formyl)-2,3'-bipyridine (**L1**) 221.05$(M+1)^+$.

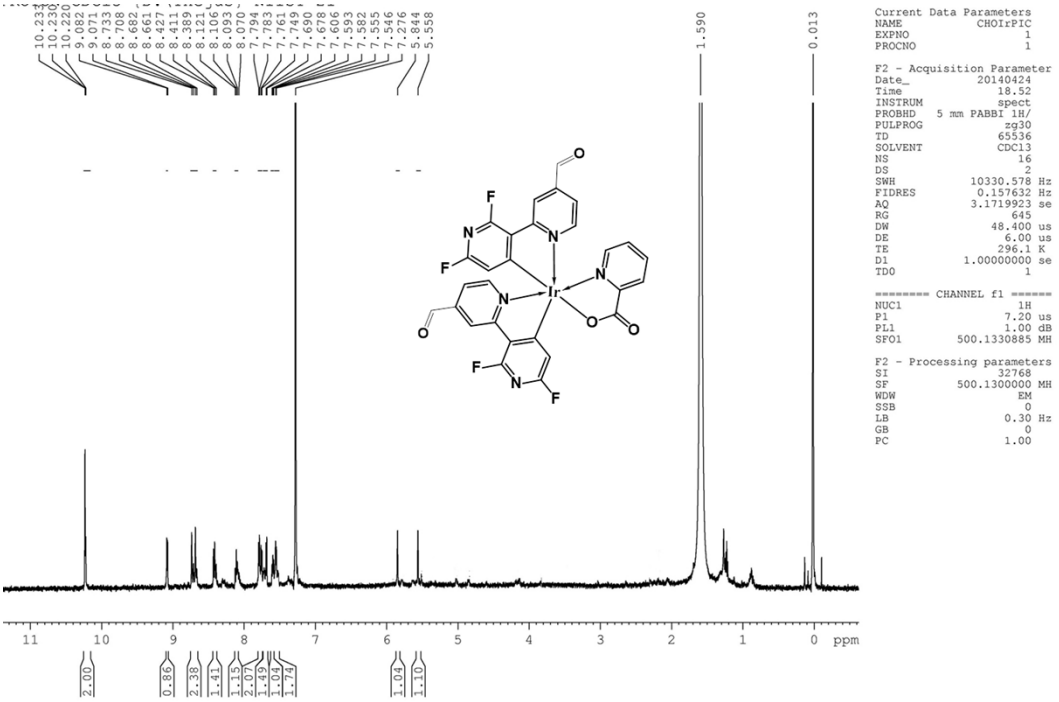

Fig. S5 ^{1}H-NMR spectrum of complex **Ir1.**

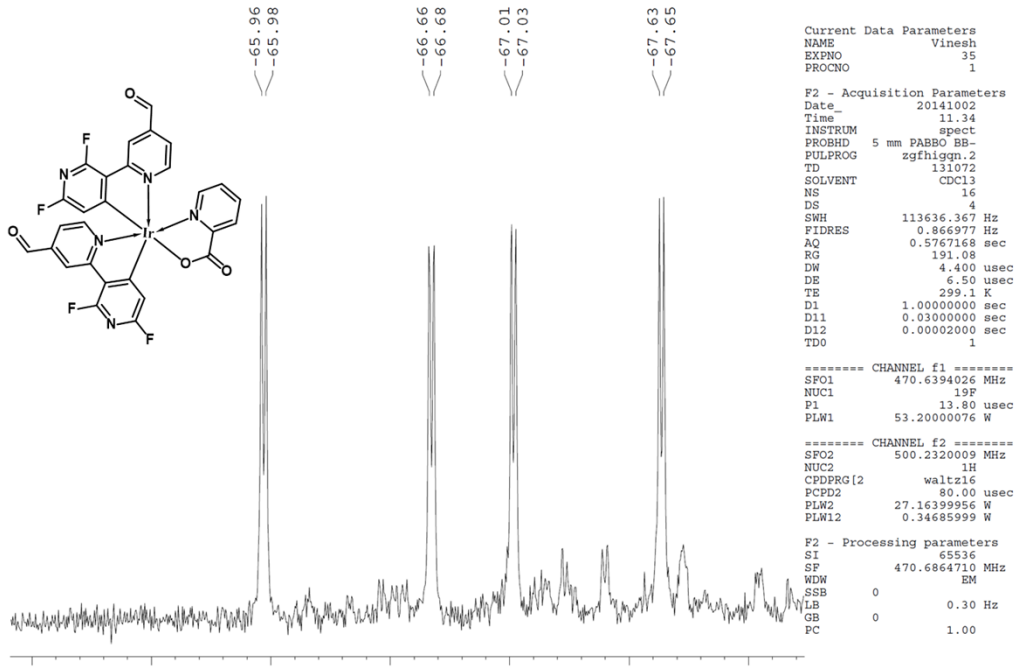

Fig. S6 ^{19}F-NMR spectrum of complex **Ir1.**

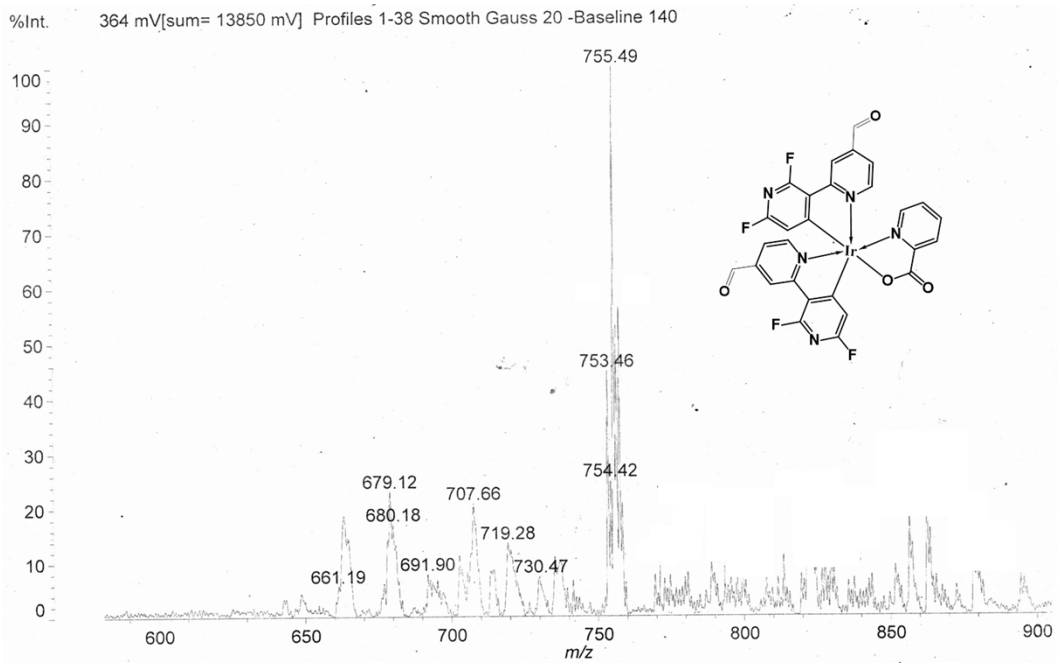

Fig. S7 MALDI-TOF spectrum of complex **Ir1** 755.49$(M+3)^{+}$.

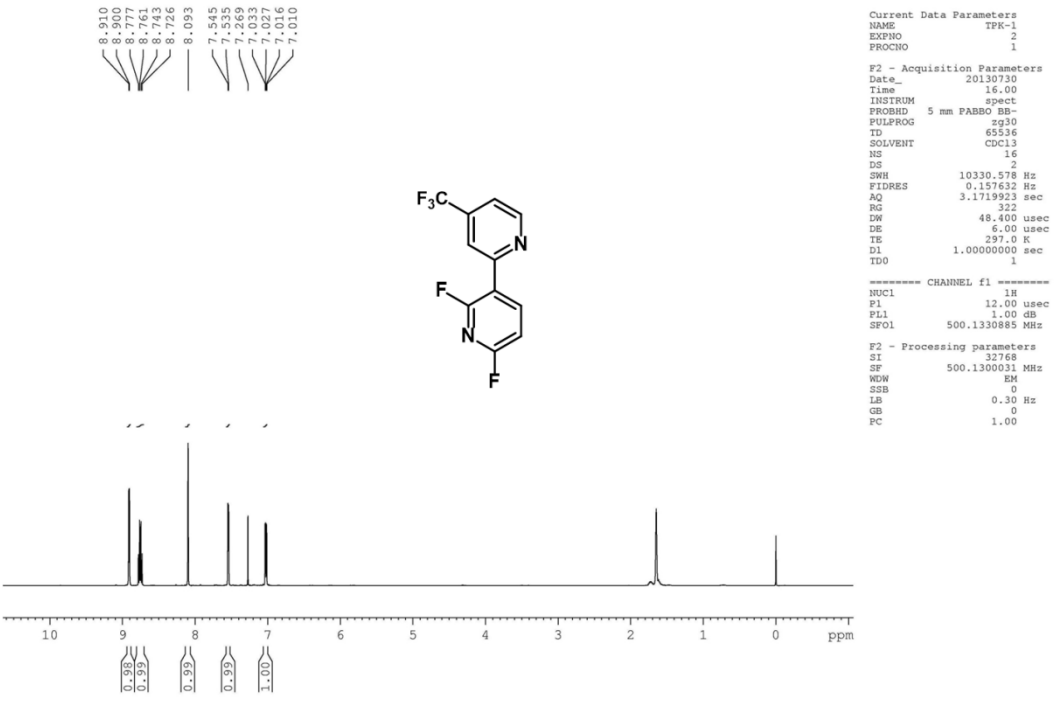

Fig. S8 ^{1}H-NMR spectrum of 2',6'-difluoro-4-(trifluoromethyl)-2,3'-bipyridine (**L2**).

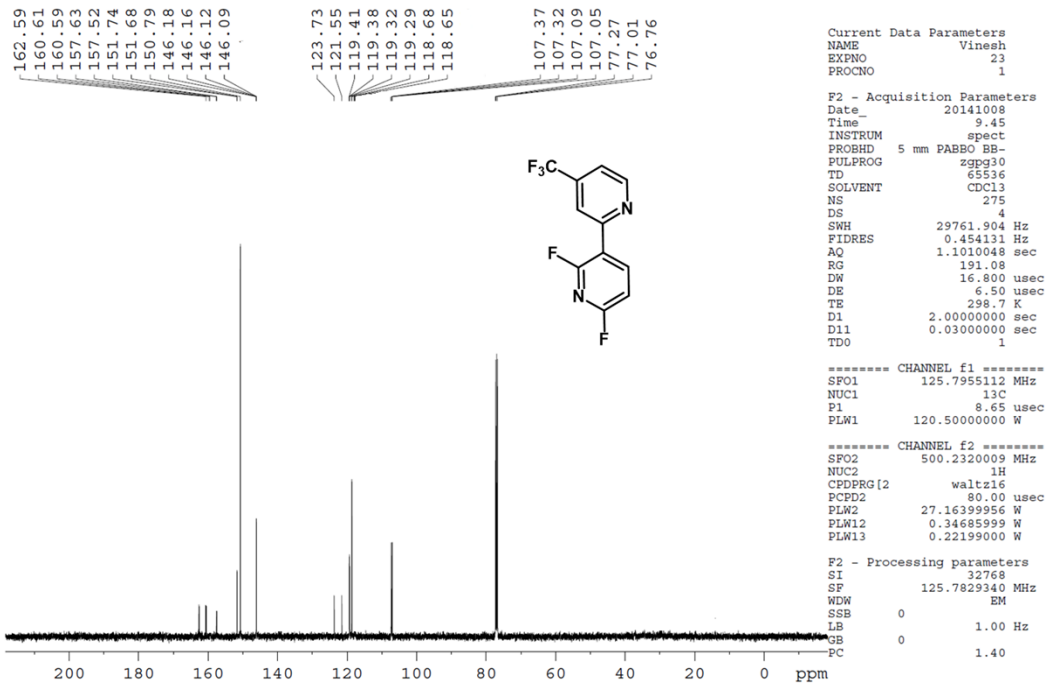

Fig. S9 ^{13}C-NMR spectrum of 2',6'-difluoro-4-(trifluoromethyl)-2,3'-bipyridine (**L2**).

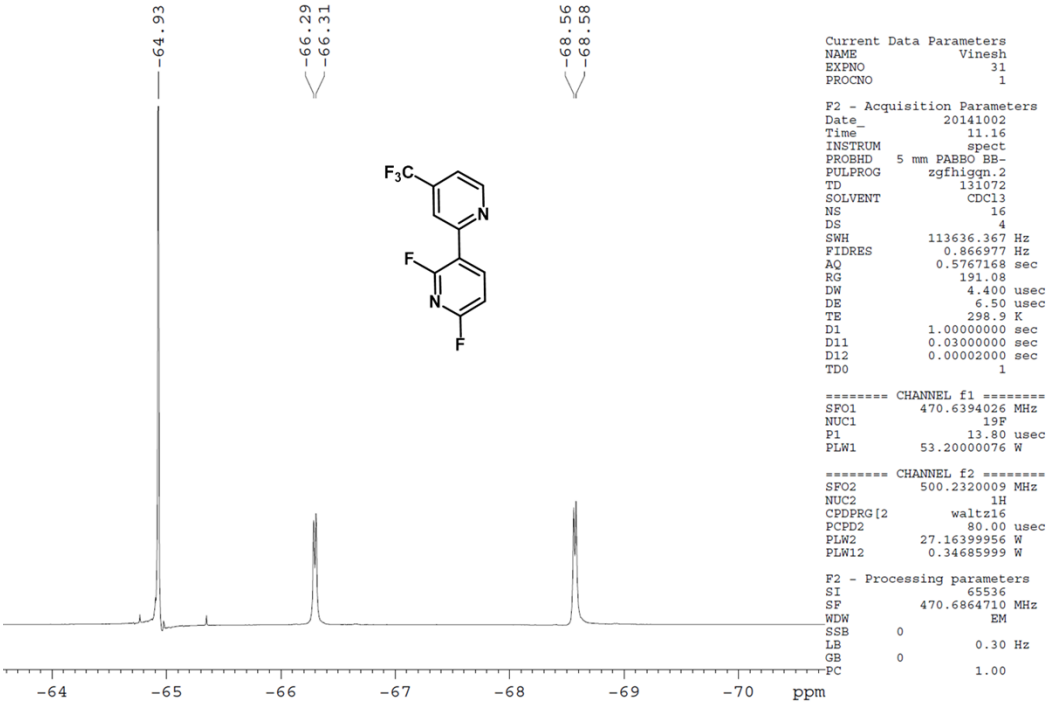

Fig. S10 ^{19}F-NMR spectrum of 2',6'-difluoro-4-(trifluoromethyl)-2,3'-bipyridine (**L2**).

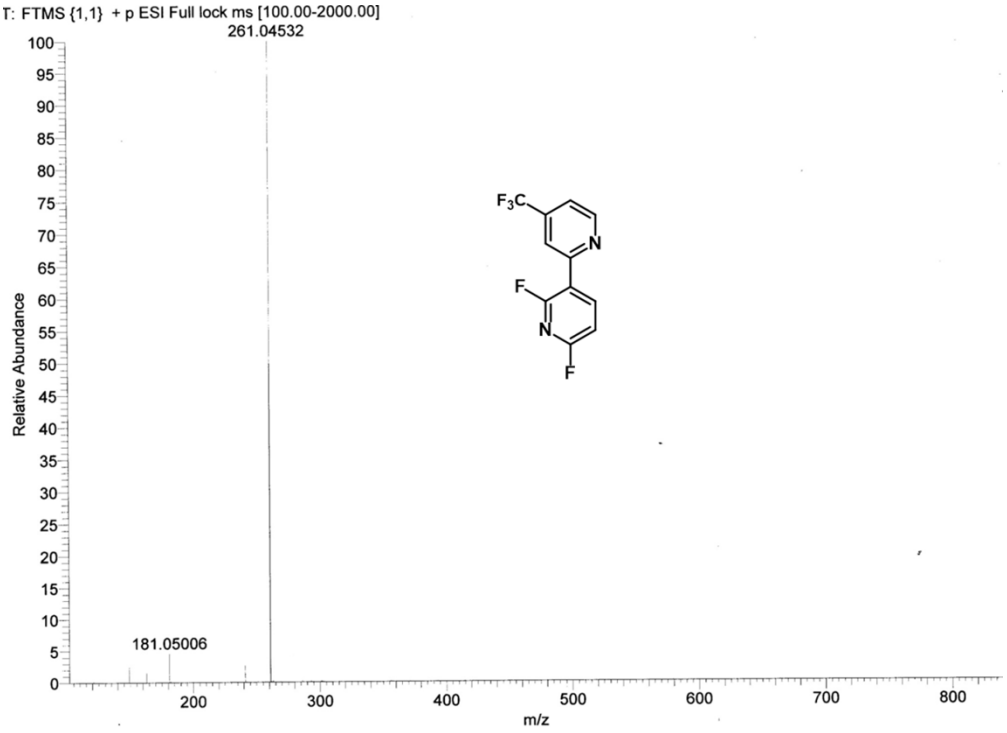

Fig. S11 ESI-MS spectrum of 2',6'-difluoro-4-(trifluoromethyl)-2,3'-bipyridine (**L2**) 261.04$(M+1)^+$.

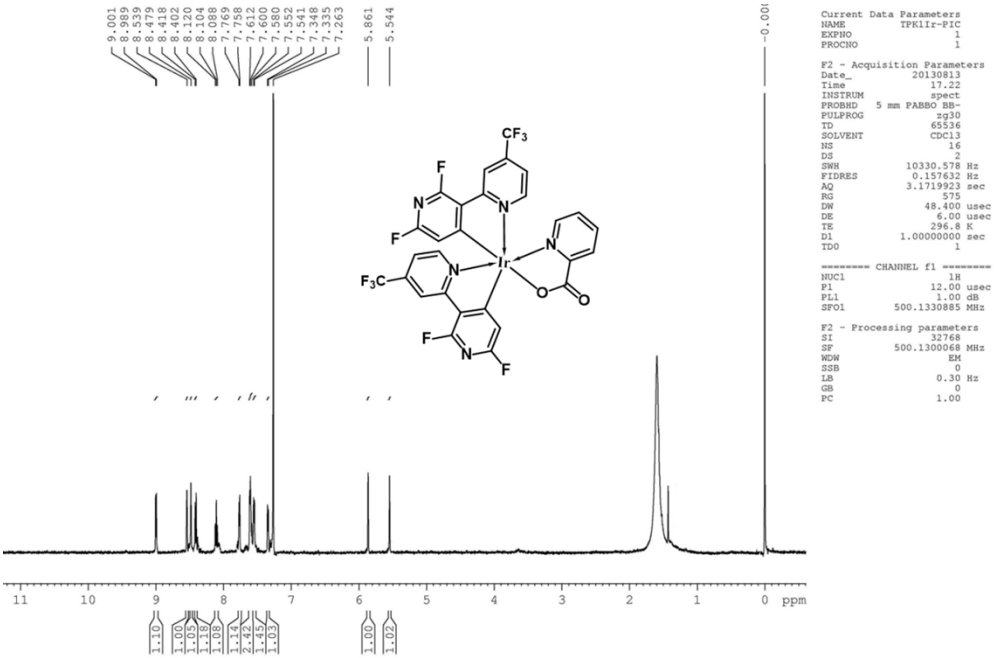


```
Current Data Parameters
NAME                  TPR1Ir-P1C
EXPNO                          1
PROCNO                         1

F2 - Acquisition Parameters
Date_                   20130813
Time                       17.22
INSTRUM                    spect
PROBHD    5 mm PABBO BB-
PULPROG                    zg30
TD                        65536
SOLVENT                   CDCl3
NS                            16
DS                             2
SWH                   10330.578 Hz
FIDRES                0.157632 Hz
AQ                    3.1719923 sec
RG                           575
DW                        48.400 usec
DE                         6.00 usec
TE                        296.8 K
D1                    1.00000000 sec
TD0                            1

======== CHANNEL f1 ========
NUC1                          1H
P1                        12.00 usec
PL1                        1.00 dB
SFO1                500.1330885 MHz

F2 - Processing parameters
SI                         32768
SF                  500.1300068 MHz
WDW                           EM
SSB                            0
LB                         0.30 Hz
GB                             0
PC                         1.00
```

Fig. S12 ^{1}H-NMR spectrum of complex **Ir2.**

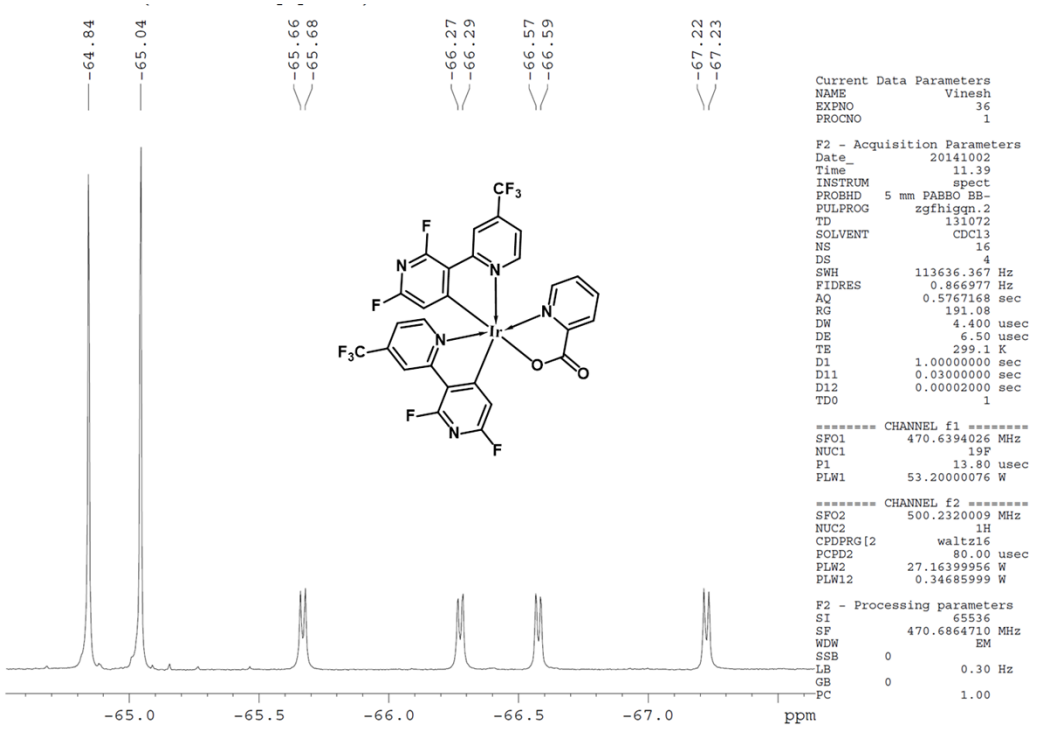

Fig. S13 ^{19}F-NMR spectrum of complex **Ir2.**

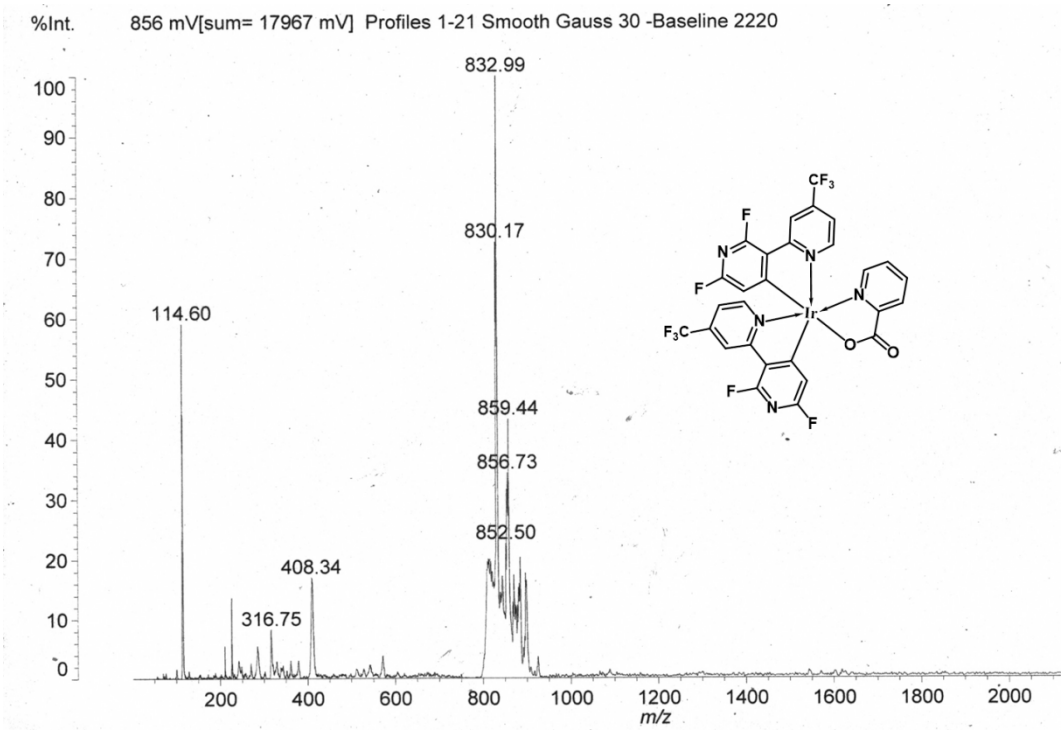

Fig. S14 MALDI-TOF spectrum of complex **Ir2**, 832.99 $(M+1)^+$.

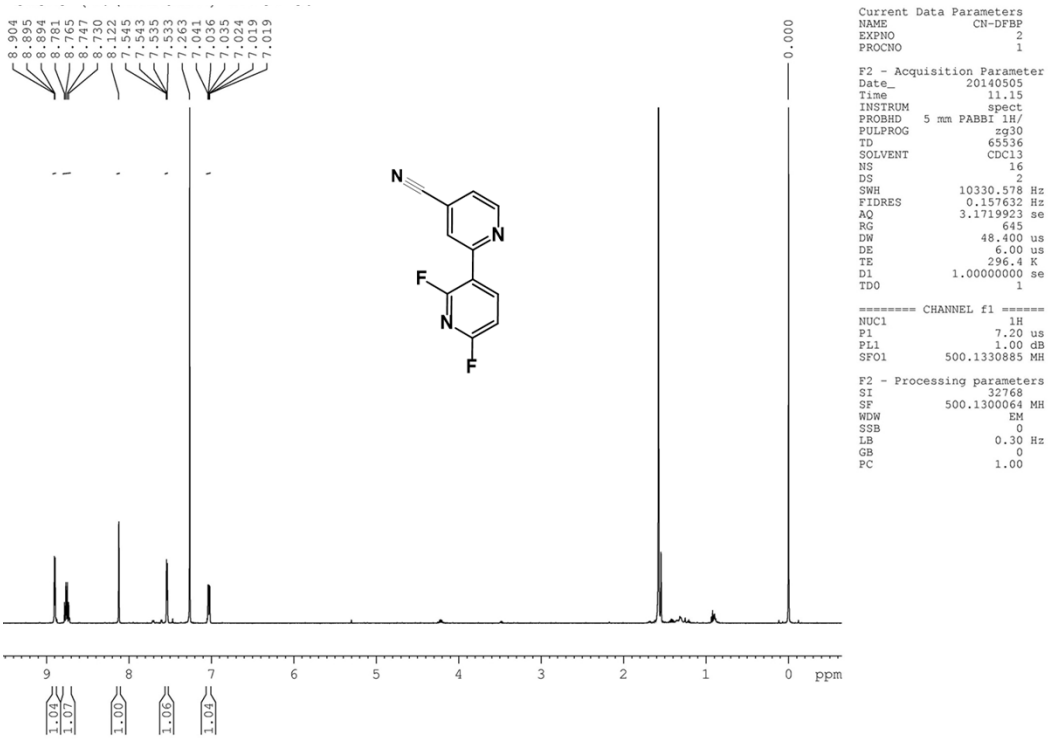

Fig. S15 [1]H-NMR spectrum of 2',6'-difluoro-4-cyano-2,3'-bipyridine (**L3**).

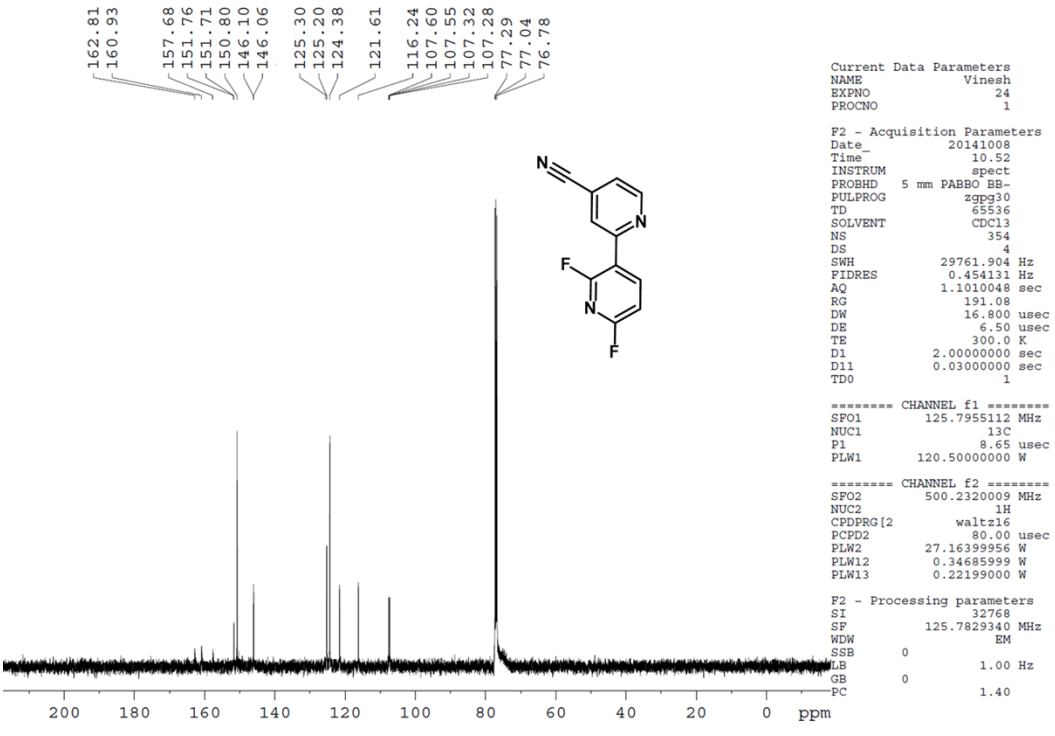

Fig. S16 [13]C-NMR spectrum of 2',6'-difluoro-4- cyano-2,3'-bipyridine (**L3**).

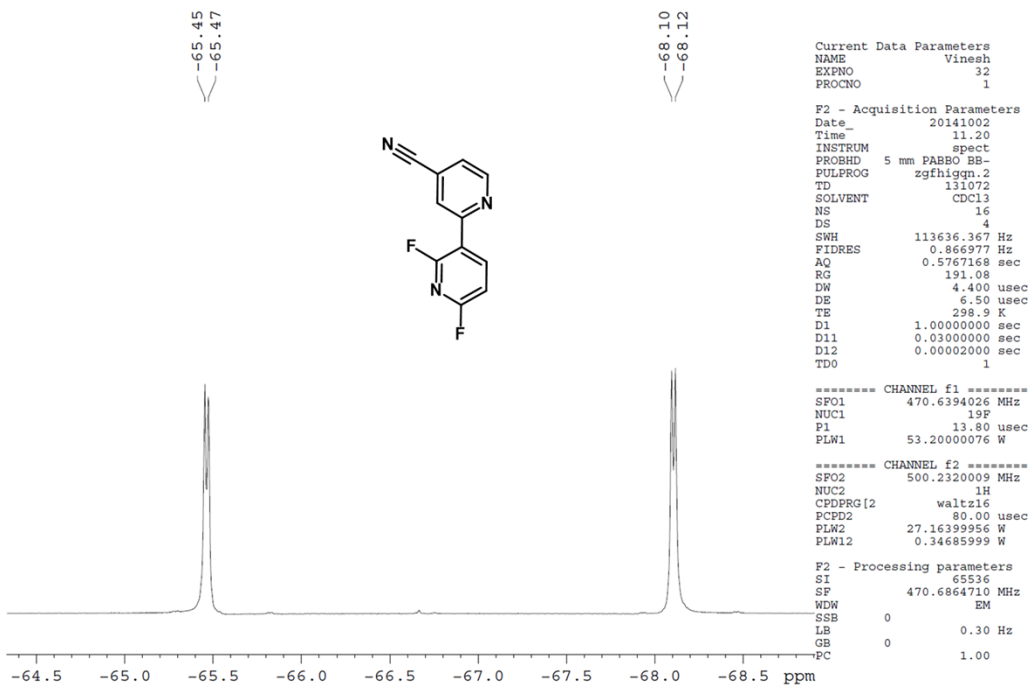

Fig. S17 ^{19}F-NMR spectrum of 2',6'-difluoro-4- cyano-2,3'-bipyridine (**L3**).

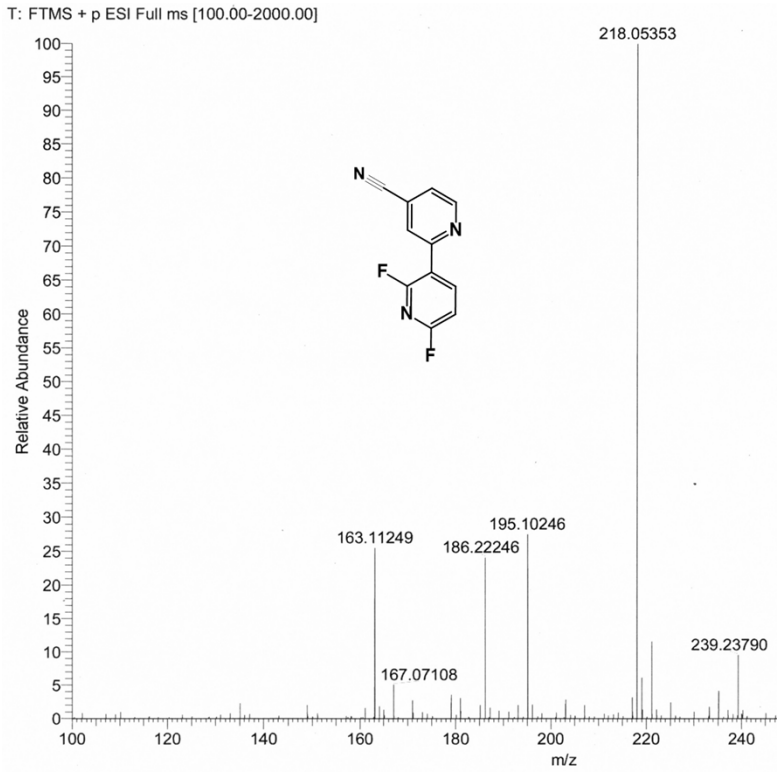

Fig. S18 ESI-MS spectrum of 2',6'-difluoro-4- cyano-2,3'-bipyridine (**L3**). 218.05$(M+1)^+$.

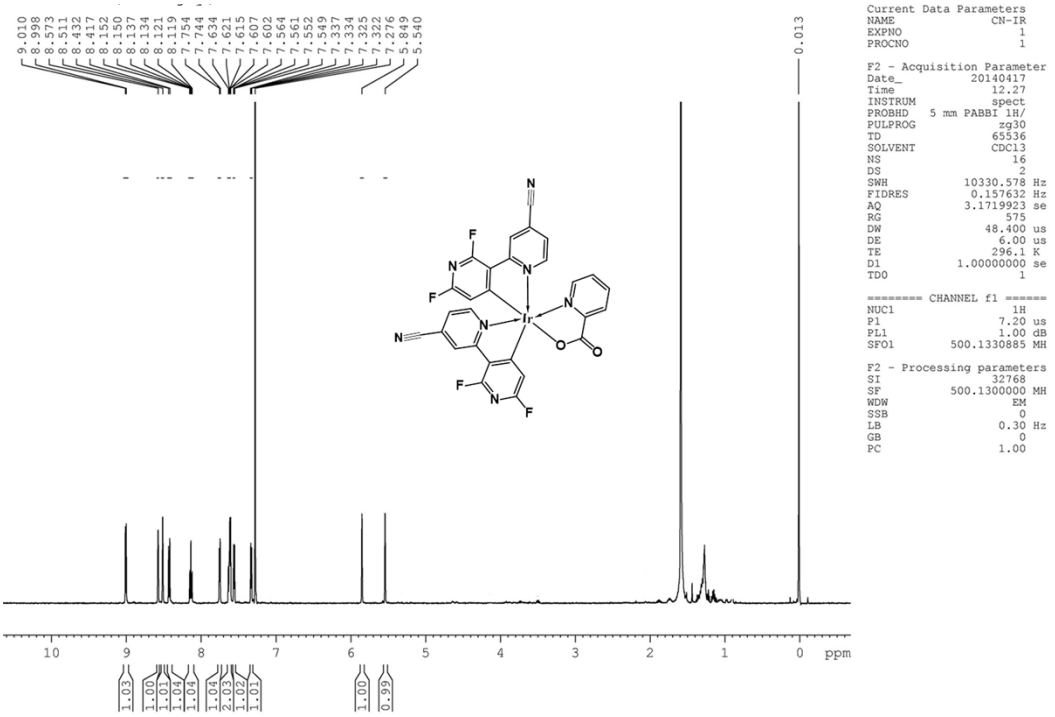

Fig. S19 [1]H-NMR spectrum of complex **Ir3.**

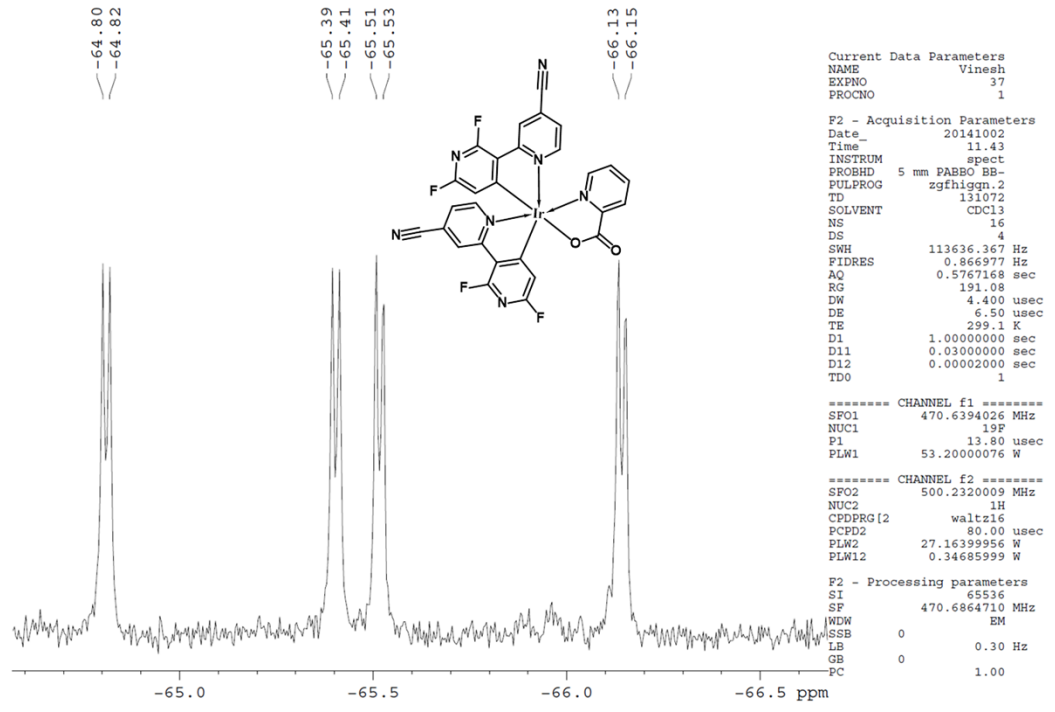

Fig. S20 [19]F-NMR spectrum of complex **Ir3.**

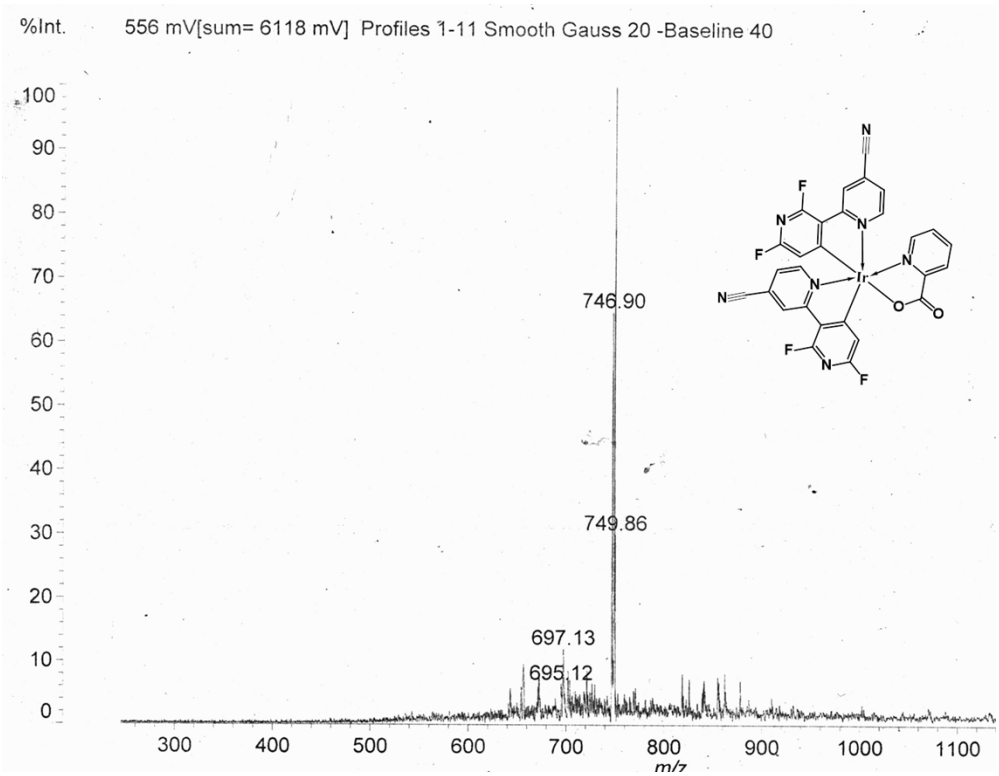

Fig. S21 MALDI-TOF spectrum of complex **Ir3**. 746.90 $(M)^+$.

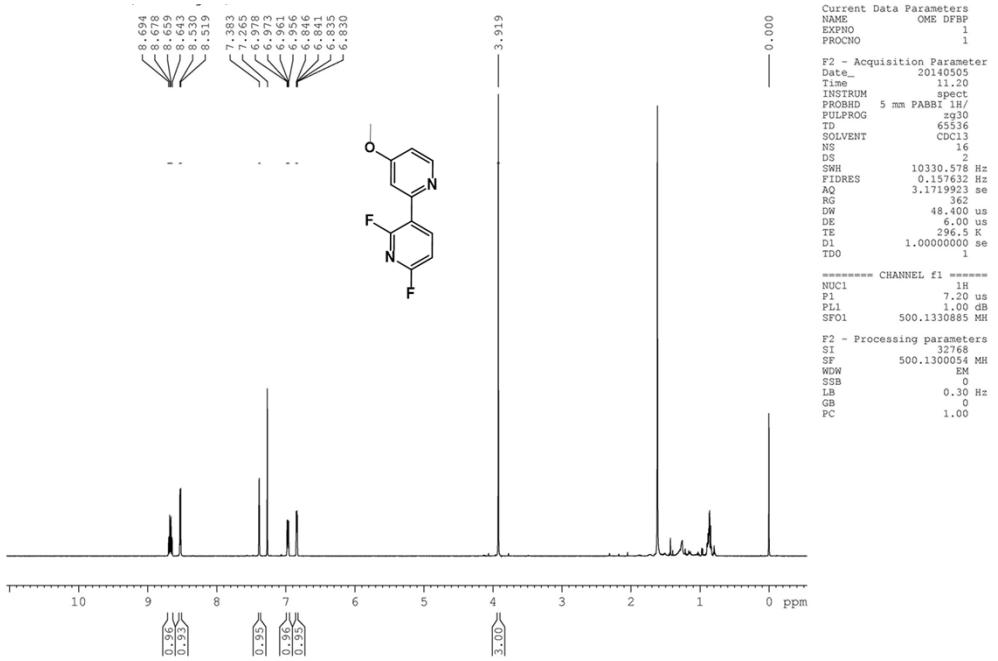

Fig. S22 ^{1}H-NMR spectrum of 2',6'-difluoro-4-methoxy-2,3'-bipyridine (**L4**).

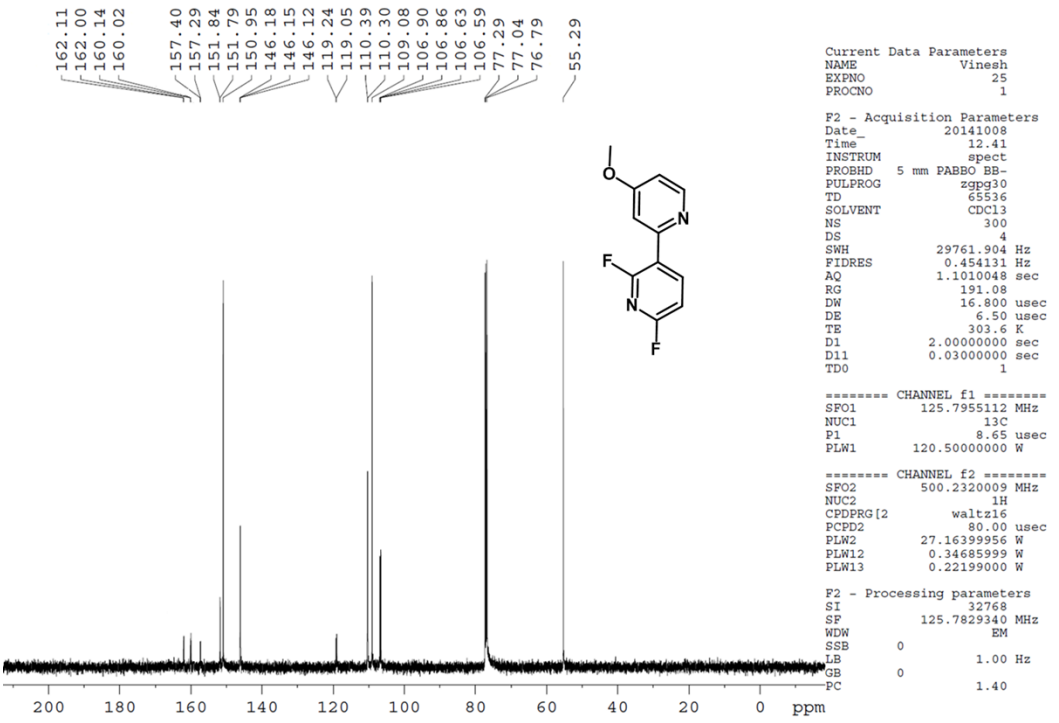

Fig. S23 ^{13}C-NMR spectrum of 2',6'-difluoro-4- methoxy-2,3'-bipyridine (**L4**).

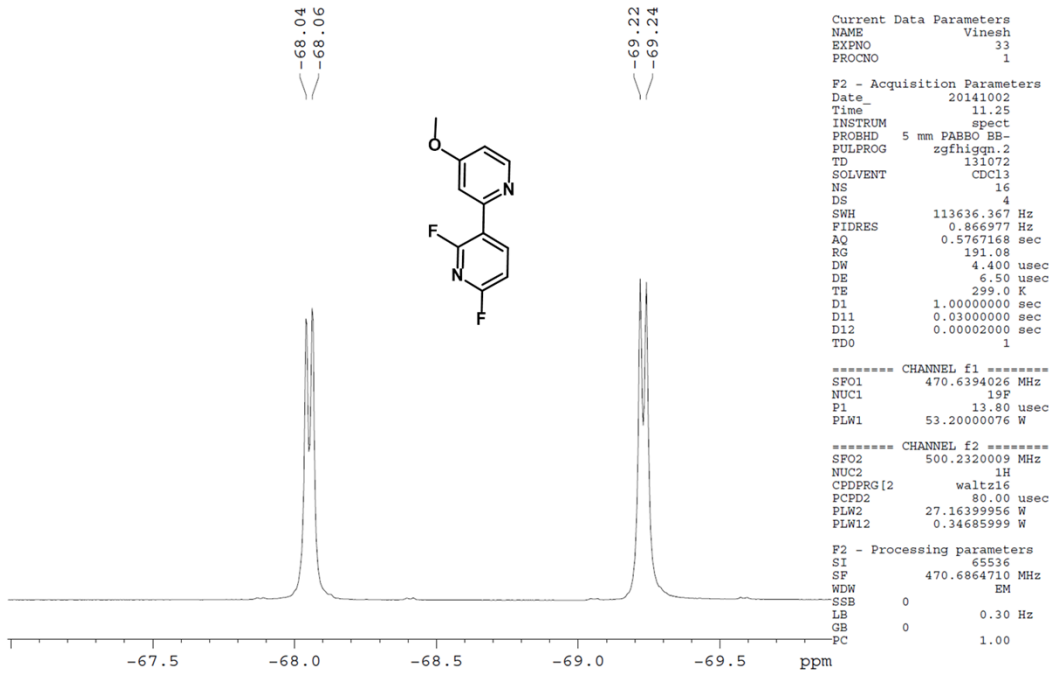

Fig. S24 ^{19}F-NMR spectrum of 2',6'-difluoro-4- methoxy-2,3'-bipyridine (**L4**).

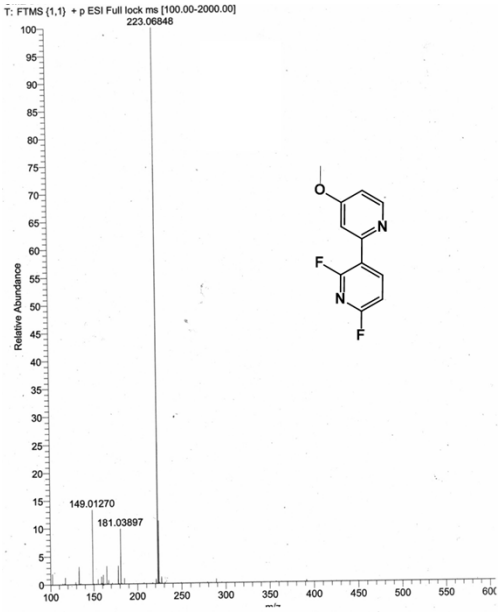

Fig. S25 ESI-MS spectrum of 2',6'-difluoro-4- methoxy-2,3'-bipyridine (**L4**). 223.06 $(M+1)^+$.

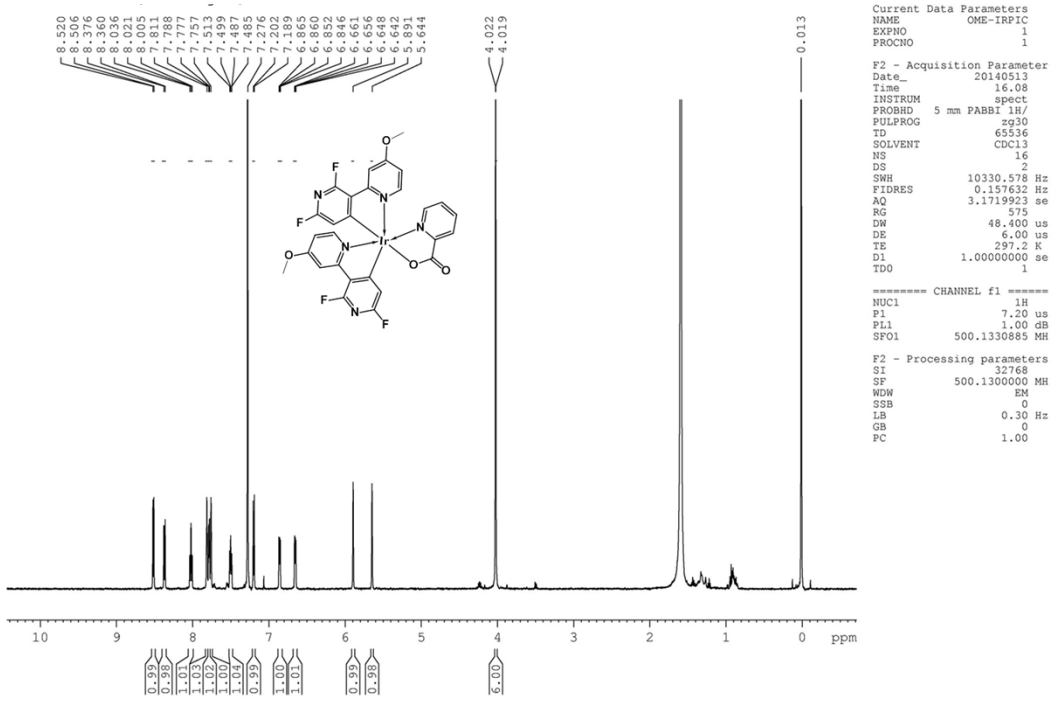

Fig. S26 ^{1}H-NMR spectrum of complex **Ir4.**

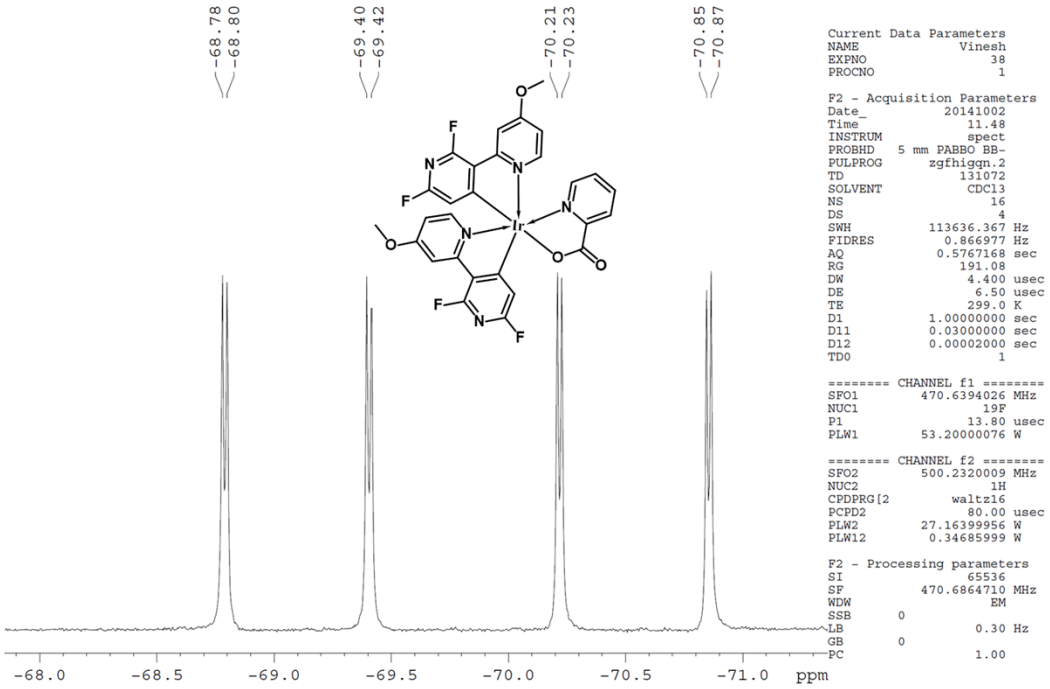

Fig. S27 ^{19}F-NMR spectrum of complex **Ir4.**

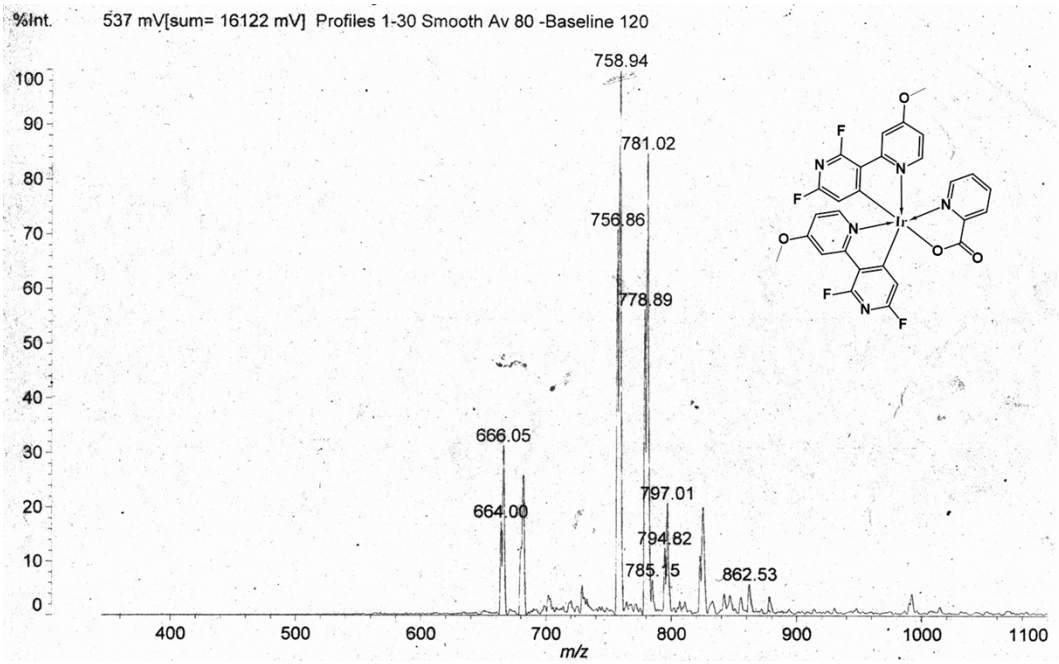

Fig. S28 MALDI-TOF spectrum of complex **Ir4**. 758.94 $(M+1)^+$.

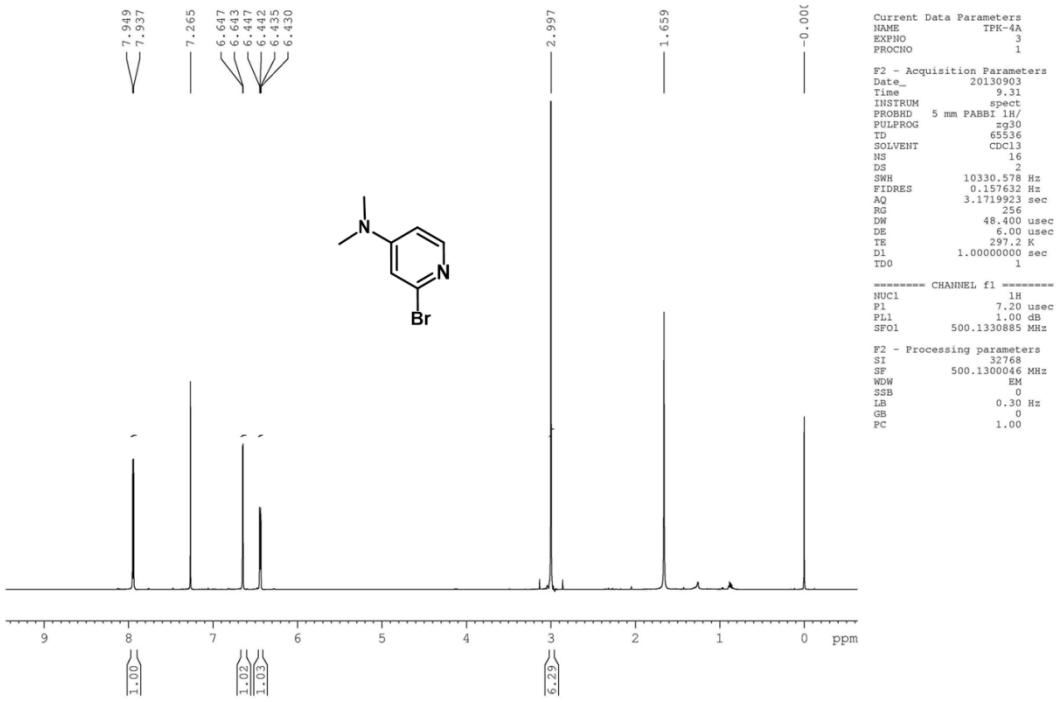

Fig. S29 ^{1}H-NMR spectrum of 2-bromo-4-N,N-dimethylaminopyridine (**L5a**).

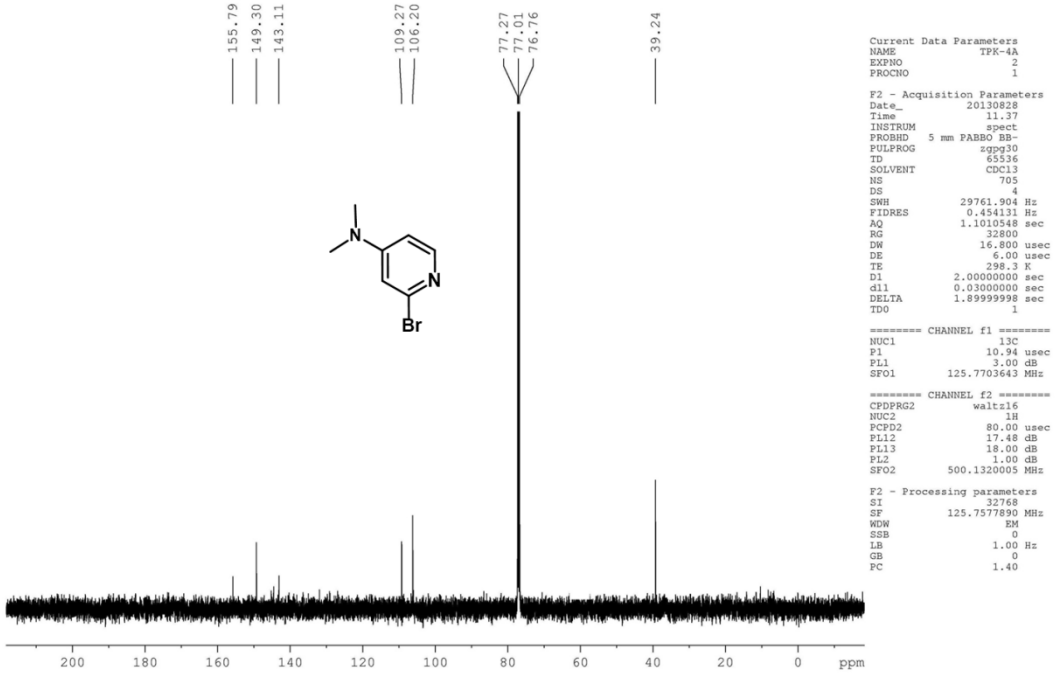

Fig. S30 ^{13}C-NMR spectrum of 2-bromo-4-N,N-dimethylaminopyridine (**L5a**).

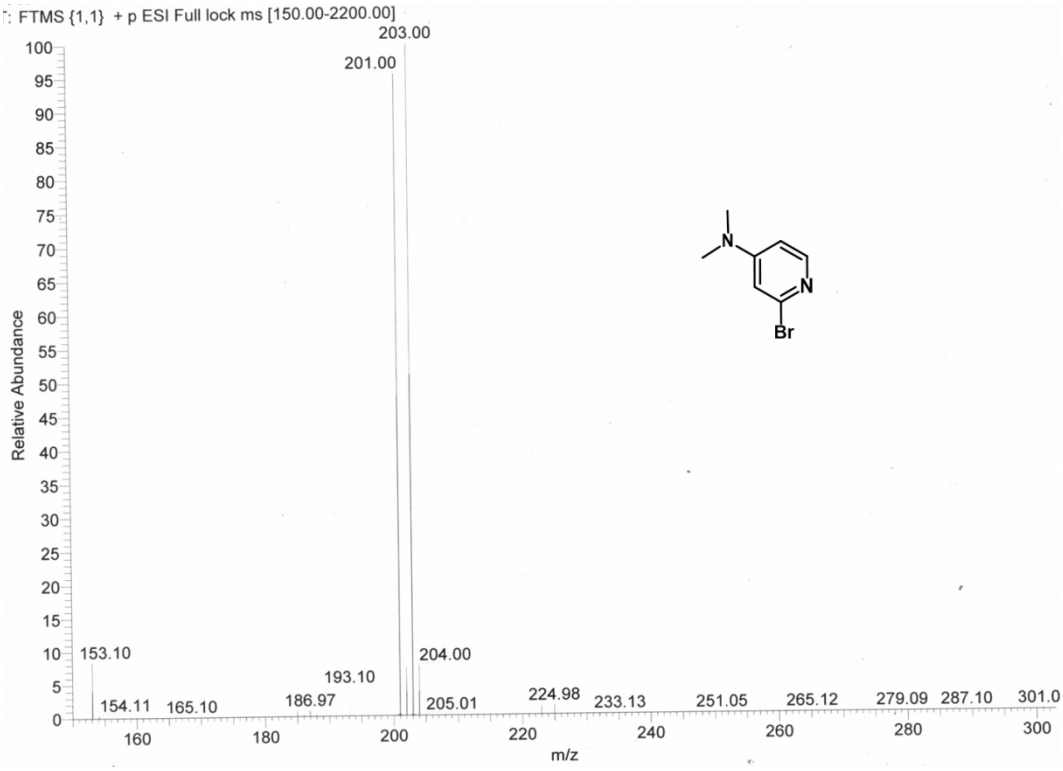

Fig. S31 ESI-MS spectrum of 2-bromo-4-N,N-dimethylaminopyridine (**L5a**) 203.00 $(M+2)^+$.

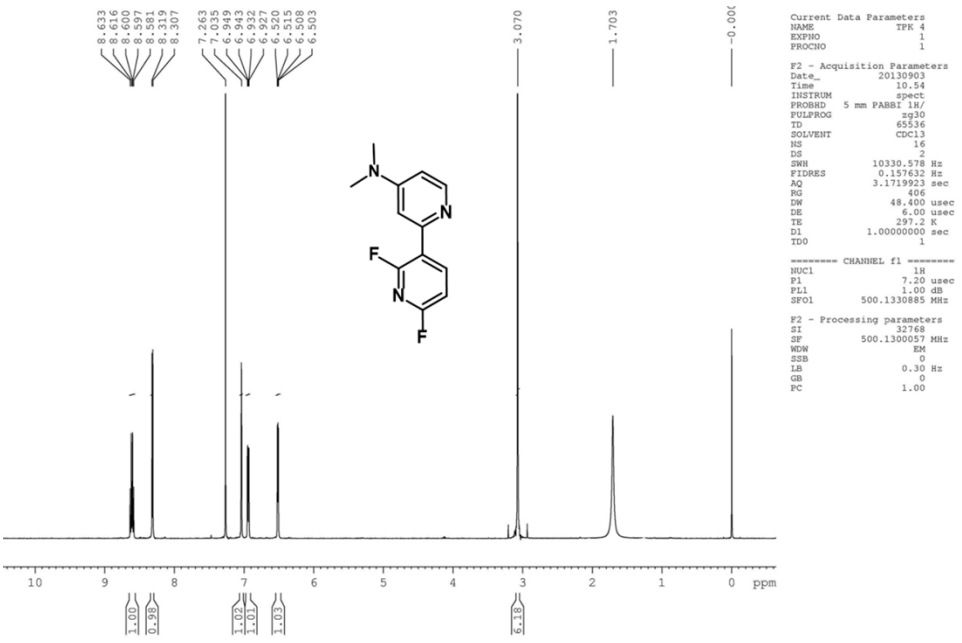

Fig. S32 ^{1}H-NMR spectrum of 2',6'-difluoro-4-(N,N-dimethylamine)-2,3'-bipyridine (**L5**).

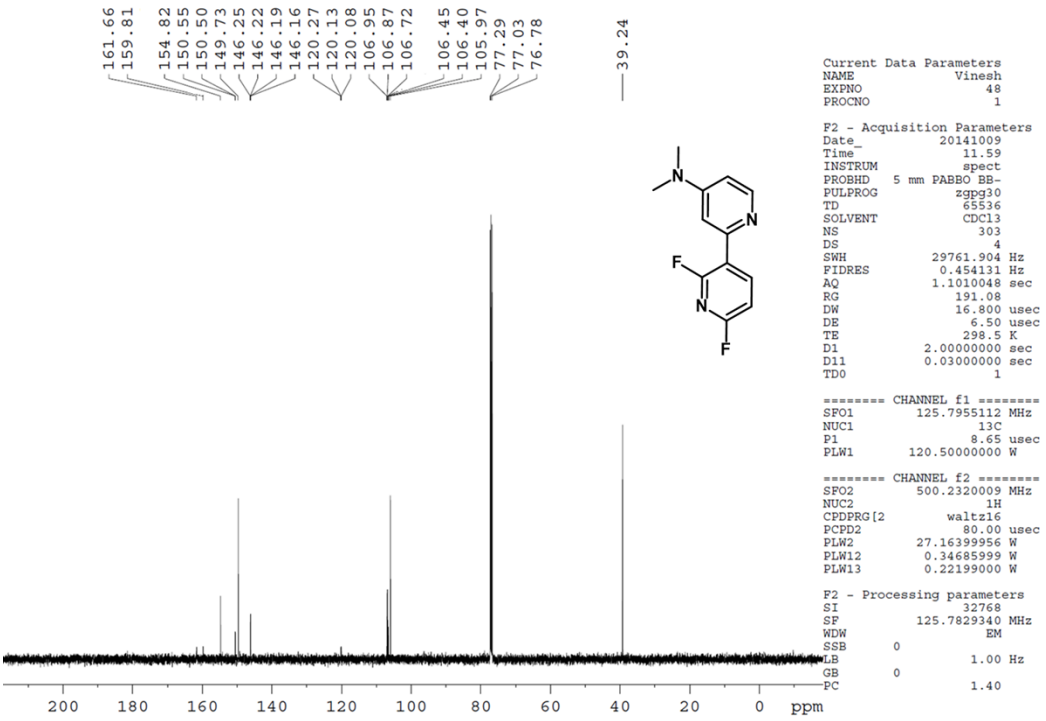

Fig. S33 ^{13}C-NMR spectrum of 2',6'-difluoro-4-(N,N-dimethylamine)-2,3'-bipyridine (**L5**).

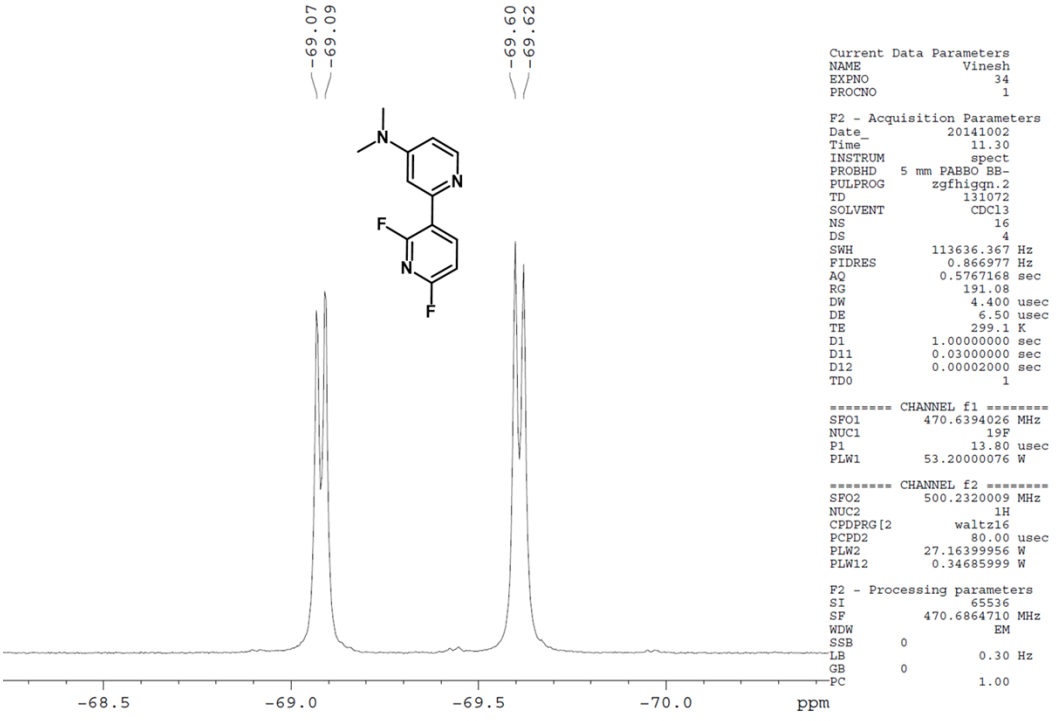

Fig. S34 ^{19}F-NMR spectrum of 2',6'-difluoro-4-(N,N-dimethylamine)-2,3'-bipyridine (**L5**).

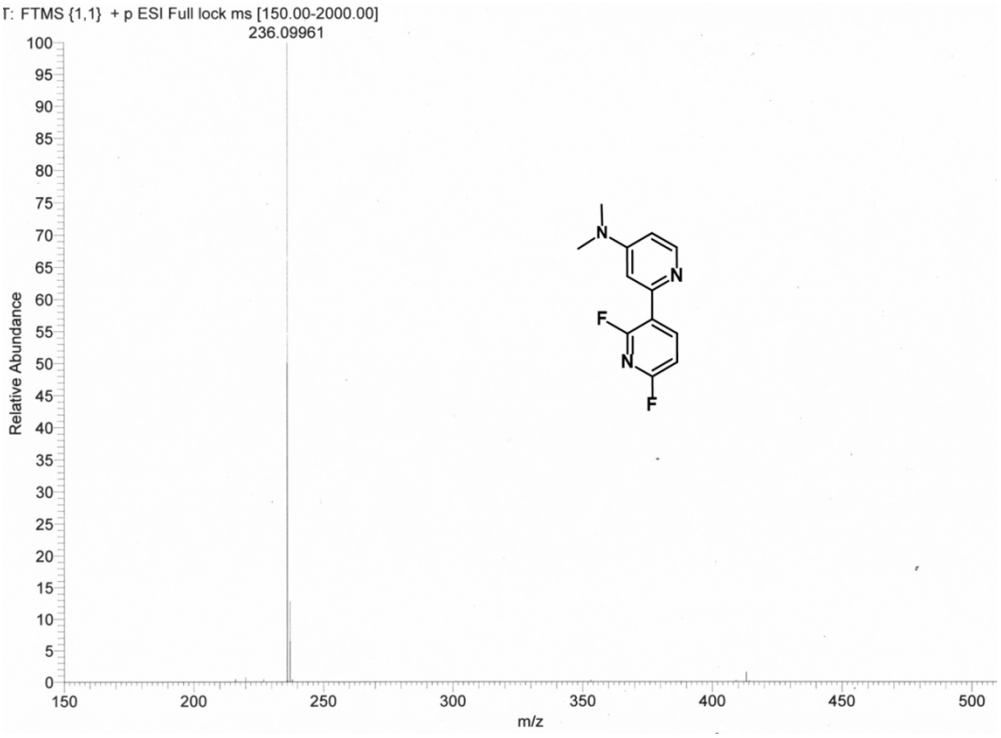

Fig. S35 ESI-MS spectrum of 2',6'-difluoro-4-(N,N-dimethylamine)-2,3'-bipyridine (**L5**) 236.09 $(M+1)^+$.

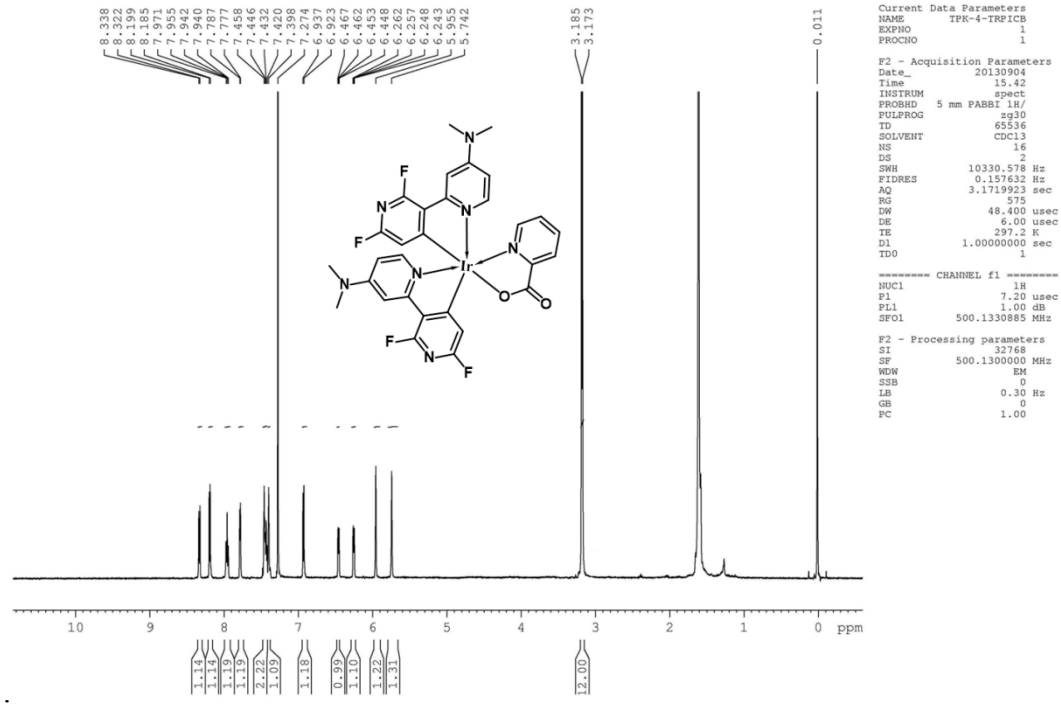

Fig. S36 ^{1}H-NMR spectrum of complex **Ir5**.

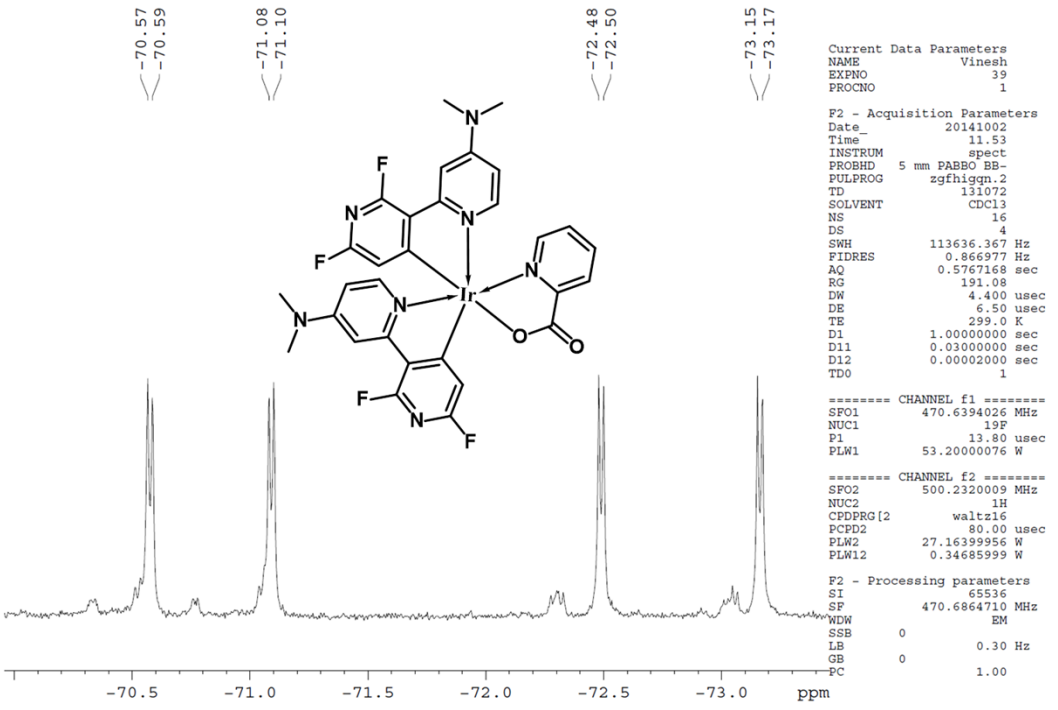

Fig. S37 ^{19}F-NMR spectrum of complex **Ir5.**

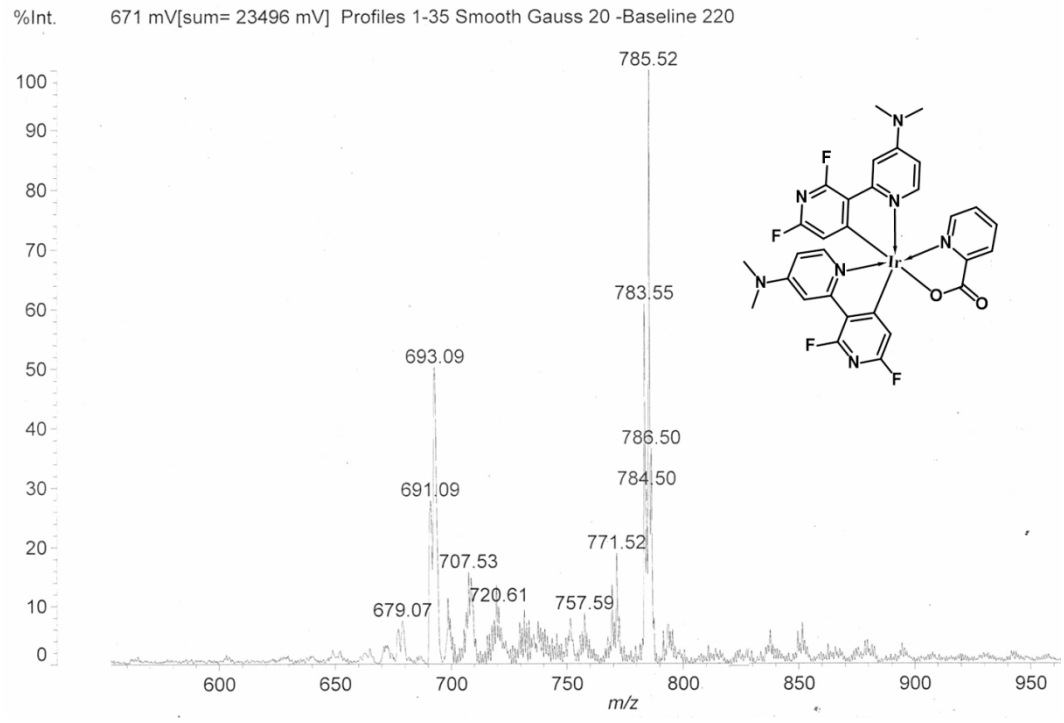

Fig. S38 MALDI-TOF spectrum of complex **Ir5**, 785.52 $(M+1)^+$.

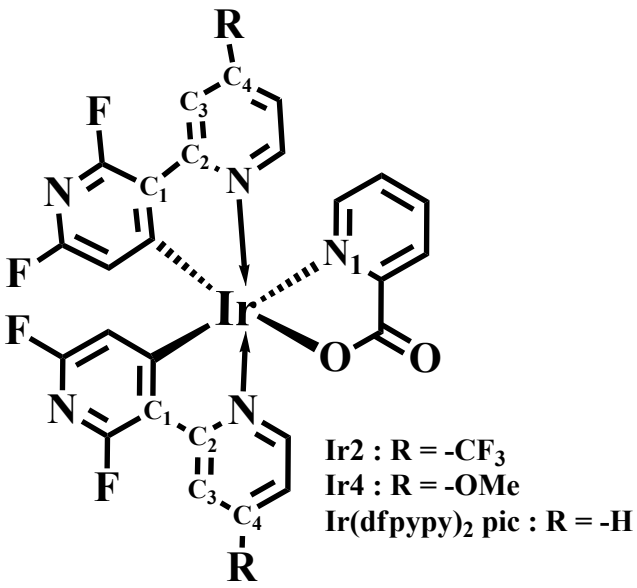

Fig. S39 General structure of the complexes shows the label used for selected atoms as used in Table 2.

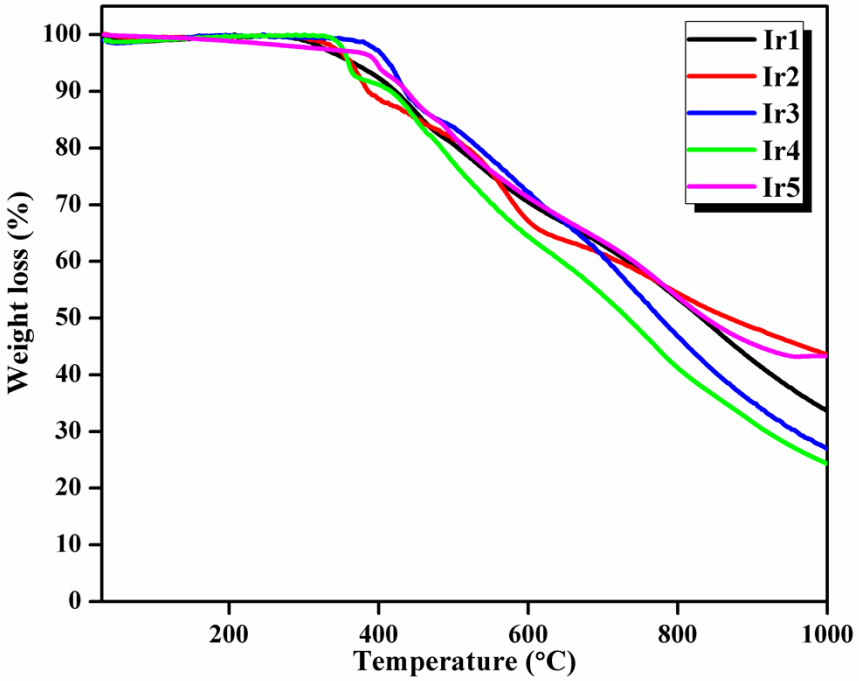

Fig. S40 Thermogravimetric curves for complex **Ir1** **Ir5** under N_2 atmosphere.

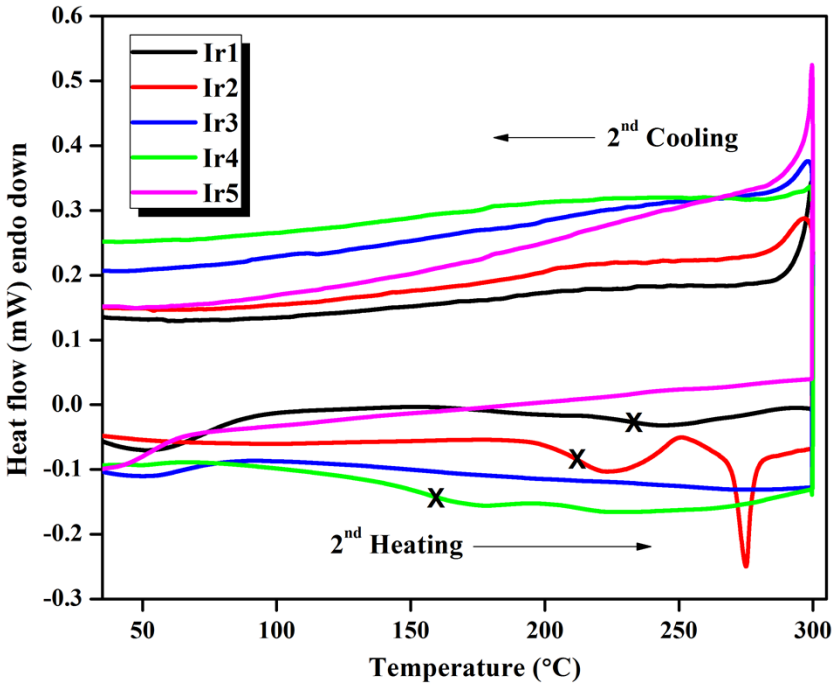

Fig. S41 Differential scanning calorimetric curves for complex **Ir1 Ir5** under N_2 atmosphere.

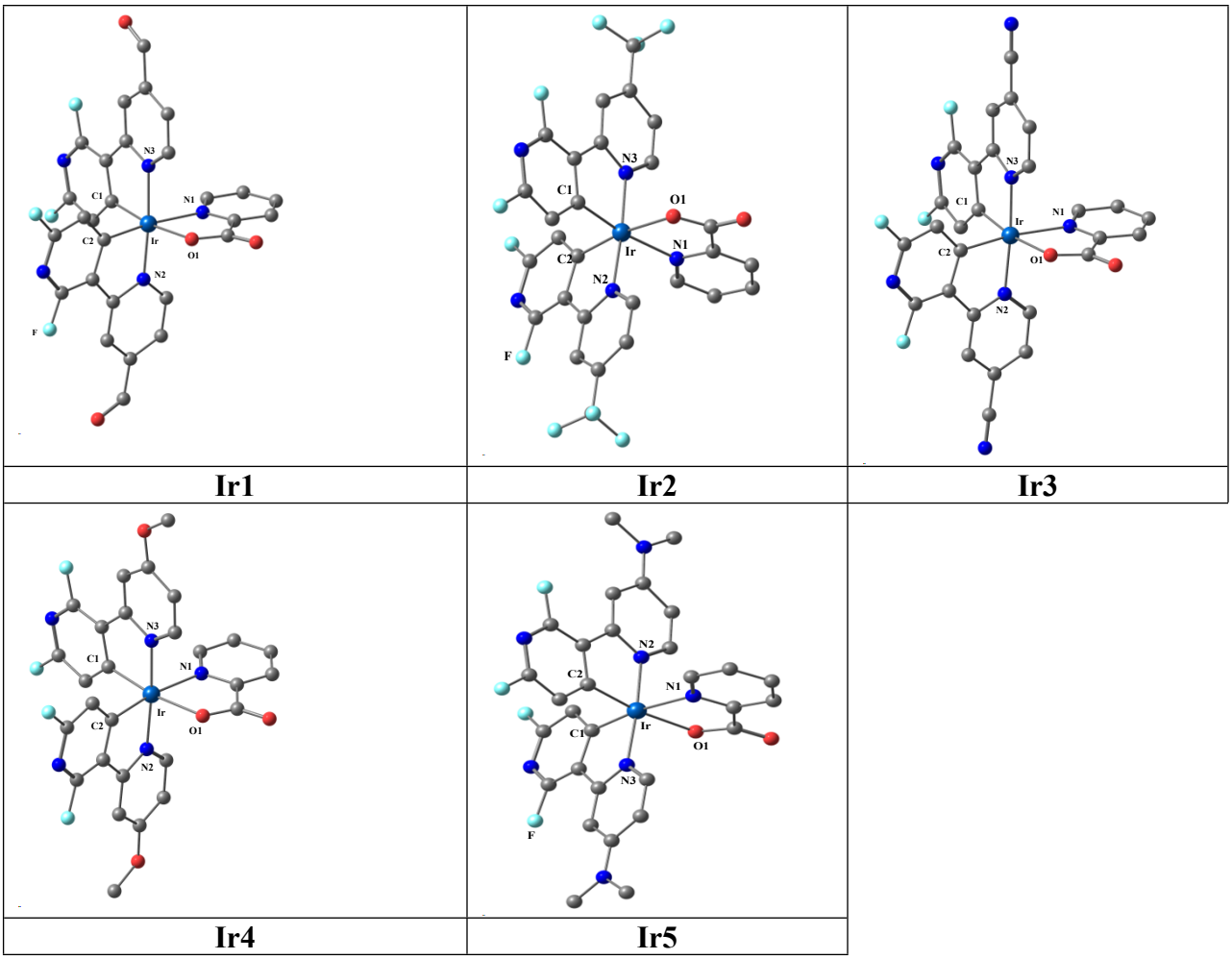

Fig. S42 Optimized geometrical structures of complex **Ir1** **Ir5**.

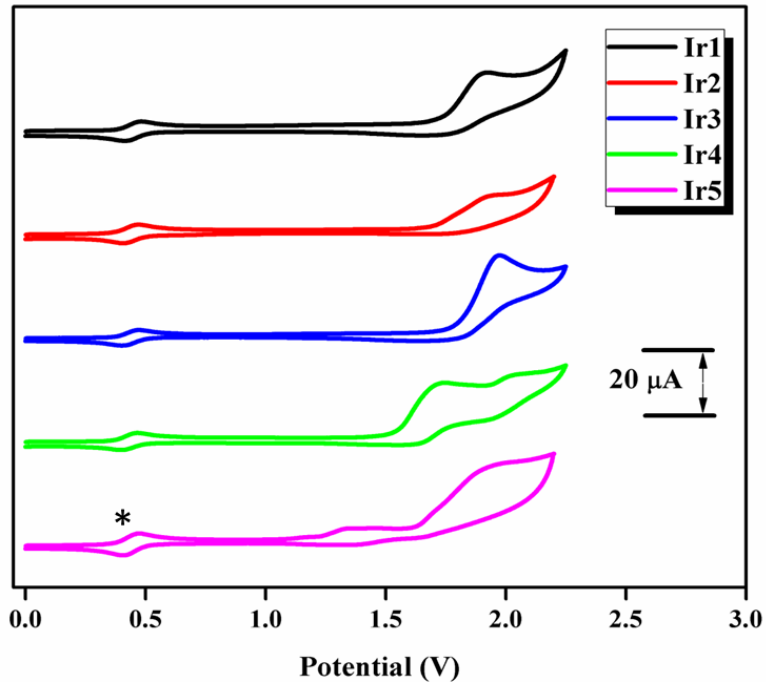

Fig. S43 Comparison of oxidation potentials (vs Ag/AgCl in CH_3CN) of **Ir1** **Ir5**, (oxidation potential $FeCp_2/FeCp_2^+$ =0.45 V, marked with asterisk).

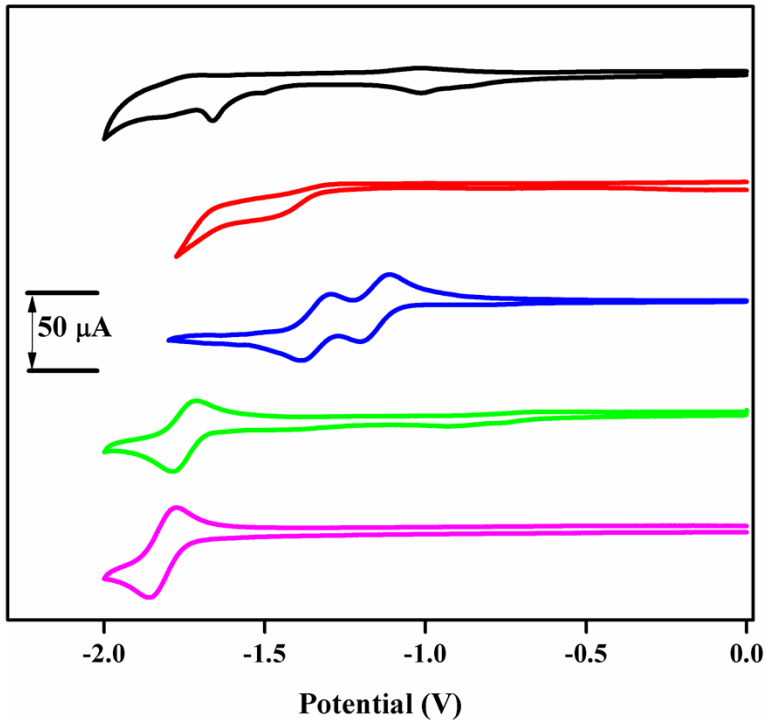

Fig. S44 Comparison of reduction potentials (vs Ag/AgCl in CH_3CN) of **Ir1** **Ir5**,

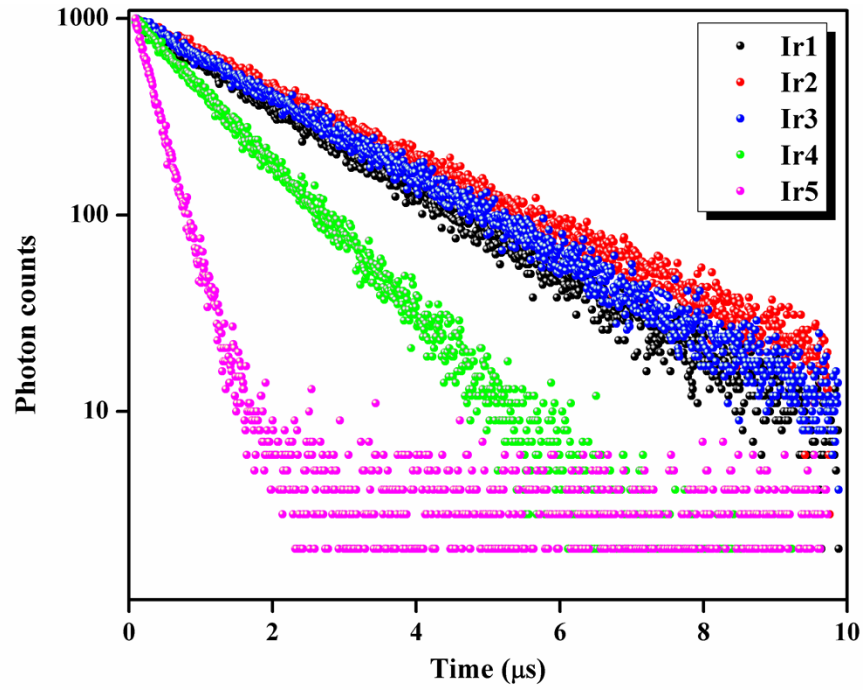

Fig. S45 Lifetime decay profiles of complex **Ir1** **Ir5** in degassed dichloromethane solution (c = 5×10^{-5} M, λ_{exc} = 375 nm) at 298 K.

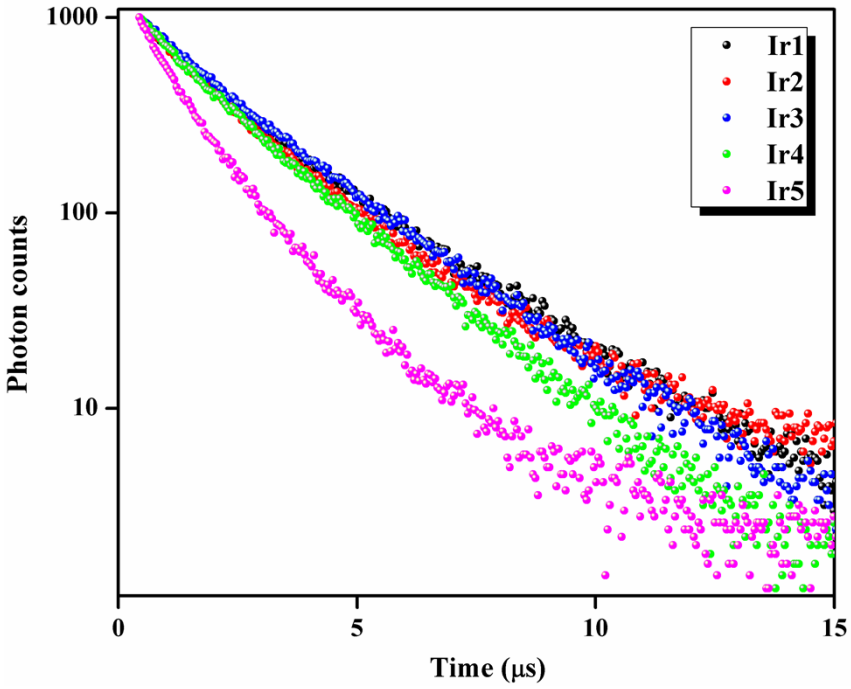

Fig. S46 Lifetime decay profiles of complex **Ir1** **Ir5** in 5 wt% doped PMMA film (λ_{exc} = 375 nm) at 298 K.

Table S1 Selected Bond Lengths for Complexes **Ir2** and **Ir4**

Selected bond lengths for **Ir2** (Å)			
Number	Atom1	Atom2	Length
1	Ir1	N6	2.150(11)
2	Ir1	N5	2.045(11)
3	Ir1	N4	2.026(10)
4	Ir1	C3A	1.966(16)
5	Ir1	C2A	1.987(10)
6	Ir1	O1	2.115(11)
Selected bond lengths for **Ir4** (Å)			
1	Ir1	N1	2.048(2)
2	Ir1	N14	2.050(2)
3	Ir1	N27	2.125(2)
4	Ir1	O33A	2.158(2)
5	Ir1	C12	1.983(2)
6	Ir1	C26	2.000(3)

Table S2 Selected Bond Angles for **Ir2**

Selected bond angles for **Ir2** (˚)				
Number	Atom1	Atom2	Atom3	Angle
1	N6	Ir1	N5	88.7(5)
2	N6	Ir1	N4	96.0(5)
3	N6	Ir1	C3A	172.5(5)
4	N6	Ir1	C2A	99.0(5)
5	N6	Ir1	O1	77.1(5)
6	N5	Ir1	N4	175.2(5)
7	N5	Ir1	C3A	96.1(5)
8	N5	Ir1	C2A	81.8(5)
9	N5	Ir1	O1	94.2(5)
10	N4	Ir1	C3A	79.1(5)
11	N4	Ir1	C2A	98.3(5)
12	N4	Ir1	O1	85.9(5)
13	C3A	Ir1	C2A	87.4(6)
14	C3A	Ir1	O1	96.8(5)
15	C2A	Ir1	O1	174.5(5)

Table S3 Selected Bond Angles for **Ir4**

Selected bond angles for **Ir4** (˚)				
Number	Atom1	Atom2	Atom3	Angle
1	C12	Ir1	C26	88.2(1)
2	C12	Ir1	N1	80.8(1)
3	C12	Ir1	N14	96.4(1)
4	C12	Ir1	N27	94.50(9)
5	C12	Ir1	O33A	169.19(9)
6	C26	Ir1	N1	93.9(1)
7	C26	Ir1	N14	80.3(1)
8	C26	Ir1	N27	174.78(9)
9	C26	Ir1	O33A	100.61(9)
10	N1	Ir1	N14	173.78(9)
11	N1	Ir1	N27	90.91(9)
12	N1	Ir1	O33A	92.24(8)
13	N14	Ir1	N27	94.89(9)
14	N14	Ir1	O33A	91.25(8)
15	N27	Ir1	O33A	77.24(8)

Table S4 Intermolecular Hydrogen Bond Interactions for **Ir2**

D-H···A	d(D-H) [Å]	d(H···A) [Å]	d(D···A) [Å]	<(DHA) [°]
C(42)-H(42A)···O(49)iv	0.93	2.66	3.299(3)	127
C(3)-H(3A)···F(50)i	0.93	3.06	3.821(5)	140
C(4)-H(4A)···F(51) ii	0.93	3.06	3.953(2)	161
C(3)-H(3A)···N(16) i	0.93	2.43	3.168(1)	136
C(17)-H(17A)···N(18)iii	0.93	2.61	3.468(7)	153

Symmetry transformations used to generate equivalent atoms: i) x,x-y,1/2+z; ii) y,-x+y,-z; iii) y,x,1/2-z; iv)1-x+y,1-x,z

Table S5 Intermolecular Hydrogen Bond Interactions for **Ir4**

D-H···A	d(D-H) [Å]	d(H···A) [Å]	d(D···A) [Å]	<(DHA) [°]
C(3)-H(3)···O(33A)i	0.95	2.81	3.597(3)	130
C(13)-H(13B)···O(17)ii	0.98	2.92	3.791(5)	138
C(90)-H(90B) ···O(17)vi	0.99	2.83	3.869(4)	161
C(20)-H(20A)···O(33B)v	0.98	2.61	3.514(4)	141
C(28)-H(28)···O(4)iv	0.95	2.48	3.281(3)	130
C(13)-H(13C)···F(22)iii	0.98	2.45	3.259(4)	130
C(13)-H(13C)···F(10)iv	0.98	2.57	3.410(4)	134
C(20)-H(20B)···F(8)vi	0.98	2.77	3.575(4)	131
C(20)-H(20B)···N(9)vi	0.98	2.67	3.642(4)	150
C(90)-H(90A)···N(23)vii	0.99	2.37	3.447(5)	171

Symmetry transformations used to generate equivalent atoms: i)1-x,2-y,1-z,-1/2+z; ii)-1+x,3/2-y,1/2+z; iii)-1+x,y,z; iv)1-x,1-y,1-z; v)1+x,y,z; vi)2-x,1-y,1-z; vii)2-x,-1/2+y,3/2-z

Table S6 Selected Bond Distances, Bond Angles and Dihedral Angles from the Optimized Ground (S_0) and Triplet State (T_1) Geometry for the Complexes **Ir1**-**Ir5** Together with the Experimental Values for **Ir2** and **Ir4**

	Ir1		**Ir2**		**Ir3**		**Ir4**		**Ir5**		**Exp**	
	S_0	**T_1**	**S_0**	**T_1**	**S_0**	**T_1**	**S_0**	**T_1**	**S_0**	**T_1**	**Ir2**	**Ir4**
Bond length (Å)												
Ir-N1	2.207	2.207	2.208	2.209	2.207	2.209	2.204	2.215	2.204	2.222	2.150	2.125
Ir-N2	2.073	2.010	2.062	2.086	2.073	2.001	2.081	2.023	2.067	2.099	2.046	2.050
Ir-N3	2.060	2.093	2.075	2.021	2.060	2.098	2.067	2.087	2.081	1.992	2.025	2.048
Ir-C1	2.006	2.011	2.006	2.002	2.006	2.011	2.003	2.005	2.005	2.016	1.965	1.983
Ir-C2	2.007	2.004	2.005	2.008	2.007	2.009	2.005	2.004	2.001	2.007	1.987	2.000
Ir-O1	2.167	2.148	2.165	2.158	2.163	2.143	2.173	2.167	2.177	2.162	2.115	2.157
Bond length(deg)												
N3-Ir-N2	175.3	175.2	175.5	175.6	175.5	175.2	175.2	175.4	175.2	175.0	175.1	173.7
N3-Ir-N1	89.0	88.3	95.7	95.5	88.9	88.3	88.8	88.4	96.1	96.0	96.0	90.9
N3-Ir-O1	92.7	92.1	88.8	90.4	92.7	91.5	93.3	92.5	88.7	92.6	85.9	92.2
N3-Ir-C2	95.2	95.0	98.0	96.9	95.3	94.9	95.3	94.5	97.8	97.0	98.3	94.0
N3-Ir-C1	80.6	80.2	80.3	81.6	80.6	80.0	80.5	80.2	80.1	81.8	79.1	80.8
Dihedral Angle (deg)												
N2-C2-Ir-N1	-64.0	-71.8	87.4	86.8	-64.3	-73.4	-65.0	-73.4	87.2	86.5	87.4	-63.9
O1-N1-Ir-C1	173.4	172.4	23.1	18.2	173.4	171.6	173.9	172.9	22.7	16.0	35.2	170.0

Table S7 Calculated Energy Levels of the HOMO, HOMO-1, HOMO-2, LUMO, LUMO+1, and LUMO+2 and Percentage of Contribution of Iridium metal (Ir), 2′,6′-difluoro-2,3′-bipyridine Derivatives and Picolinate (pic) Ligands

Complex		E (eV)	Ir	Substituted pyridyl moiety	Difluoropyridyl moiety	pic
Ir1	LUMO+3	-1.969	1.71	57.94	30.83	13.16
	LUMO+2	-2.224	2.97	3.67	6.79	92.60
	LUMO+1	-2.974	4.7	88.90	10.11	1.01
	LUMO	-3.038	4.89	88.42	9.77	1 52
	HOMO	-6.422	51.20	7.77	29.44	11.59
	HOMO-1	-6.591	45.11	10.32	62.81	26.71
	HOMO-2	-6.823	6.54	16.57	53.50	30.18
Ir2	LUMO+3	-1.91	1.9	57.81	12.81	27.9
	LUMO+2	-2.25	3.3	4.14	2.45	92.2
	LUMO+1	-2.45	5.4	75.08	15.09	1.9
	LUMO	-2.53	5.3	75.08	41.70	2.9
	HOMO	-6.45	52.1	10.21	27.08	11.1
	HOMO-1	-6.63	47.1	13.82	13.96	25.2
	HOMO-2	-6.89	7.7	26.38	41.70	24.8
Ir3	LUMO+3	-2.174	1.55	64.81	21.81	11.83
	LUMO+2	-2.368	3.03	4.89	0.83	91.24
	LUMO+1	-2.942	5.32	84.19	9.22	1.27
	LUMO	-3.015	5.53	82.61	9.82	2.04
	HOMO	-6.645	51.75	6.79	28.31	13.14
	HOMO-1	-6.782	45.37	9.68	14.77	30.18
	HOMO-2	-7.019	1.53	4.62	15.43	78.42
Ir4	LUMO+3	-1.420	1.95	18.49	2.90	76.66
	LUMO+2	-1.506	5.11	65.34	26.99	2.56
	LUMO+1	-1.661	3.48	58.70	31.15	6.67
	LUMO	-1.875	3.47	5.41	1.70	89.42
	HOMO	-5.978	52.56	8.11	26.59	12.74
	HOMO-1	-6.040	50.11	14.73	13.60	21.55
	HOMO-2	-6.383	49.95	21.18	11.25	17.63
Ir5	LUMO+3	-1.05	2.6	14.60	2.37	80.4
	LUMO+2	-1.18	3.7	63.56	30.00	1.6
	LUMO+1	-1.32	3.5	55.83	27.81	6.6
	LUMO	-1.55	2.8	3.34	0.87	93.0
	HOMO	-5.62	45.0	30.43	9.86	14.6
	HOMO-1	-5.66	53.4	10.28	24.79	11.4
	HOMO-2	-5.86	40.8	52.16	3.85	3.0

Table S8 Calculated Absorption of **Ir1-Ir5** in CH_2Cl_2 Media at TD-B3LYP Level together with Experimental Values

	State	λ(nm)/E(eV)	Oscillator	Main configuration	Assign	λ_{exp} (nm)
Ir1	S_1	434/2.86	0.0111	H→L (90%)	CHOdfbpy/ Ir → CHOdfbpy (ILCT/ MLCT/LLCT)	
	S_4	385/3.22	0.1709	H-1→L+1(84%)	CHOdfbpy/ Ir → CHOdfbpy (ILCT/ MLCT)	387
	S_9	357/3.47	0.0796	H-3→L+1(58%)	CHOdfbpy / Ir/ pic→ CHOdfbpy (MLCT/ LLCT)	
	S_{11}	341/3.63	0.1191	H-4→L (82%)	CHOdfbpy/ Ir → CHOdfbpy (MLCT/ LLCT)	334
	S_{16}	318/3.90	0.1416	H→L+3(90%)	CHOdfbpy/ Ir → CHOdfbpy (ILCT/ MLCT/ LLCT)	
	S_{22}	292/4.24	0.0560	H-2→L+2 (62%)	CHOdfbpy → pic (LLCT)	
	S_{27}	280/4.42	0.0572	H-2→L+3(45%)	CHOdfbpy → CHOdfbpy (LLCT)	
	S_{30}	278/4.45	0.0203	H-4→L+2(62%)	CHOdfbpy/ Ir→ pic (MLCT/ LLCT)	274
Ir2	S_1	372/ 3.32	0.0016	H→L (95%)	CF_3dfbpy/ Ir/ pic→ CF_3dfbpy/ Ir (ILCT/ MLCT)	377
	S_4	343/ 3.61	0.1132	H-1→L+1(71%)	Ir /CF_3dfbpy / pic→ CF_3dfbpy (ILCT/ MLCT/ LLCT)	
	S_7	319/3.88	0.0771	H-2→L+1(36%)	CF_3dfbpy / Ir/ pic→ CF_3dfbpy/ Ir (ILCT/ MLCT/ LLCT)	
	S_{12}	303/4.09	0.1714	H-4→L (42%)	Ir/ pic→ CF_3dfbpy (MLCT/ LLCT)	
	S_{20}	282/4.39	0.1353	H-1→L+4(74%)	Ir/ CF_3dfbpy / pic→ CF_3dfbpy (ILCT/ MLCT/ LLCT)	
	S_{28}	261/4.73	0.0538	H-6→L (46%)	Ir/ CF_3dfbpy / pic→ CF_3dfbpy (ILCT/ MLCT/ LLCT)	255
	S_{30}	259/4.79	0.0414	H-6→L+1(71%)	Ir/ CF_3dfbpy / pic→ CF_3dfbpy/ Ir (ILCT/ MLCT/ LLCT)	
Ir3	S_1	415/2.98	0.0191	H→L (93%)	Ir/ CNdfbpy → CNdfbpy (MLCT/ ILCT/ LLCT)	
	S_3	388/3.19	0.0008	H-1→L (81%)	Ir/ CNdfbpy → CNdfbpy (MLCT/ LLCT)	391
	S_4	370/3.35	0.1723	H-1→L+1(78%)	Ir/ CNdfbpy → CNdfbpy (ILCT/ MLCT)	
	S_7	337/3.67	0.0850	H-3→L (60%)	Ir/ CNdfbpy → CNdfbpy (MLCT/ LLCT)	
	S_{10}	327/3.79	0.1204	H-4→L(69%)	Ir/ CNdfbpy → CNdfbpy (LLCT/ MLCT)	321
	S_{14}	314/3.94	0.1212	H→L+3(71%)	Ir/ CNdfbpy → pic (LLCT/ ILCT/MLCT)	
	S_{19}	292/4.25	0.0777	H-1→L+4(83%)	Ir/ CNdfbpy → CNdfbpy (ILCT/ MLCT)	
	S_{28}	272/4.55	0.0647	H-2→L+4 (46%)	CNdfbpy / pic→ CNdfbpy (ILCT/ LLCT)	
	S_{30}	269/4.60	0.0108	H-3→L+3 (72%)	Ir/ CNdfbpy → pic (MLCT/ LLCT)	260

	State	λ(nm)/E(eV)	Oscillator	Main configuration	Assign	λexp (nm)
Ir4	S_1	349/3.55	0.0047	H→L (97%)	Ir/OMedfbpy→pic (MLCT/LLCT)	355
	S_4	331/3.75	0.0757	H-1→L+1(82%)	Ir/OMedfbpy →OMedf bpy (MLCT/LLCT/ILCT)	
	S_7	317/3.91	0.0823	H-2→L(56%)	Ir/OMedfbpy /pic→ pic (LLCT/MLCT/ILCT)	
	S_{24}	265/4.67	0.2847	H-1→L+5 (34%)	Ir/OMedfbpy → OMedfbpy (MLCT/LLCT/ILCT)	
	S_{27}	259/4.78	0.0925	H-2→L +5 (39%)	Ir/OMedfbpy /pic → OMedfbpy (MLCT/LLCT)	
	S_{29}	256/4.83	0.1589	H-2→L+5(33%)	Ir/OMedfbpy /pic → OMedfbpy (MLCT/LLCT)	
	S_{30}	254/4.88	0.0073	H-3→L+3(58%)	Ir/ pic→ pic (ILCT/ MLCT)	254
Ir5	S_1	365/3.39	0.0122	H→L (92%)	Ir/ NMe_2dfbpy/ pic→ pic (MLCT/ LLCT)	
	S_3	351/3.53	0.0385	H-1→L (94%)	Ir/ NMe_2dfbpy/ pic→ pic (MLCT/ LLCT)	345
	S_6	332/3.73	0.1390	H→L+2(81%)	Ir/ NMe_2dfbpy/ pic→ NMe_2dfbpy/ pic (MLCT/ LLCT/ILCT)	
	S_{12}	302/4.10	0.0351	H-1→L+3(59%)	Ir/ NMe_2dfbpy/ pic→ NMe2dfbpy/ pic (MLCT/ LLCT/ILCT)	
	S_{21}	277/4.46	0.0953	H-1→L+4(33%)	Ir/ NMe_2dfbpy/ pic→ NMe_2dfbpy/ pic (ILCT/ MLCT/ LLCT)	
	S_{26}	269/4.59	0.1854	H→L+5(21%)	Ir/ NMe_2dfbpy/ pic→ NMe_2dfbpy (MLCT/ ILCT/ LLCT)	
	S_{29}	265/4.67	0.3187	H-1→L+5(24%)	Ir/ NMe_2dfbpy/ pic→ NMe_2dfbpy (MLCT/ ILCT/ LLCT)	265
	S_{30}	263/ 4.70	0.0788	H→L+6(22%)	Ir/ NMe_2dfbpy/ pic→ NMe_2dfbpy/ Ir (MLCT/ ILCT/ LLCT)	

Table S9 Calculated singlet-triplet splitting energy at the B3LYP/6-31G* level.

Complexes	S_1	T_1	ΔE_{S1-T1}
Ir1	2.561	2.054	0.507
Ir2	2.914	2.232	0.682
Ir3	2.706	2.112	0.594
Ir4	3.103	2.339	0.764
Ir5	3.050	2.329	0.721